Output only modal identification and structural damage detection using time frequency & wavelet techniques

S. Nagarajaiah[1†] and B. Basu[2‡]

1. *Dept. of Civil & Environmental Eng. and Dept. of Mechanical Eng. & Material Sc., Rice University, Houston, Texas, U.S.A.*

2. *Dept. of Civil, Structural, & Environmental Eng., Trinity College Dublin, Dublin 2, Ireland*

Abstract: The primary objective of this paper is to develop output only modal identification and structural damage detection. Identification of multi-degree of freedom (MDOF) linear time invariant (LTI) and linear time variant (LTV—due to damage) systems based on Time-frequency (TF) techniques—such as short-time Fourier transform (STFT), empirical mode decomposition (EMD), and wavelets—is proposed. STFT, EMD, and wavelet methods developed to date are reviewed in detail. In addition a Hilbert transform (HT) approach to determine frequency and damping is also presented. In this paper, STFT, EMD, HT and wavelet techniques are developed for decomposition of free vibration response of MDOF systems into their modal components. Once the modal components are obtained, each one is processed using Hilbert transform to obtain the modal frequency and damping ratios. In addition, the ratio of modal components at different degrees of freedom facilitate determination of mode shape. In cases with output only modal identification using ambient/random response, the random decrement technique is used to obtain free vibration response. The advantage of TF techniques is that they are signal based; hence, can be used for output only modal identification. A three degree of freedom 1:10 scale model test structure is used to validate the proposed output only modal identification techniques based on STFT, EMD, HT, wavelets. Both measured free vibration and forced vibration (white noise) response are considered. The secondary objective of this paper is to show the relative ease with which the TF techniques can be used for modal identification and their potential for real world applications where output only identification is essential. Recorded ambient vibration data processed using techniques such as the random decrement technique can be used to obtain the free vibration response, so that further processing using TF based modal identification can be performed.

Keywords: Time-frequency methods; short time Fourier transform; Hilbert transform; wavelets; modal identification; output only; structural health monitoring; damage detection

1   Introduction

Modal identification of structural systems is a key step in the process of structural identification, structural health monitoring and damage detection. It essentially requires an inverse problem to be solved from a measured or recorded response of the structure under ambient or dynamic loading such as earthquakes, wind and waves. The aim is to estimate properties of the structure such as natural frequencies, mode shapes, energy dissipation characteristics and strength and stiffness deterioration due to damage.

System identification of structures has classically been performed in two different paradigms: (i) time domain analysis and (ii) frequency domain analysis. Several approaches to time domain system identification have been developed like state estimation using a Kalman filter, stochastic analysis and modeling, recursive modeling and least squares method. Recently, system identification and fault detection techniques are also being developed. The work of Nagarajaiah and coworkers has led to the development of a new interaction matrix formulation and input error formulation (Koh *et al*., 2005a,b, 2008), based on the concept of analytical redundancy, to detect and isolate the damage/fault in structural members, sensors, and actuators in a structural system (Li *et al*., 2007; Chen and Nagarajaiah, 2007, 2008a,b) . The new techniques can detect the presence of fault/damage in a structure (level 1), locate the member/sensor/actuator where fault/damage is located (level 2), and determine the time instants of occurrence (level 3). The resulting error function would indicate real time failure/damage of a member, sensor or actuator. The interaction matrix technique allows the development of input-output equations that are only influenced by

one target input. These input-output equations serve as an effective tool to monitor the integrity of each member, sensor or actuator regardless of the status of the others. The procedure requires the knowledge of the analytical model of the healthy system being tested, so the analytical redundancy can be experimentally predetermined through input-output based system identification. Additionally, the authors have developed an ARMarkov observer bank algorithm to detect the extent of damage—level 4 (Dharap *et al.*, 2006). The authors have also shown experimentally that the proposed algorithms successfully identify failures of actuators or sensors that are attached to the truss structure in tests on the NASA 8-bay 4 meter long truss (Koh *et al.*, 2005a; Li *et al.*, 2007). Considering the limited number of measurements and the complexity of the structure, test results ensure the capability of the proposed procedure in detecting and isolating the simultaneously and arbitrarily occurring multiple failures. In addition, new time segmented system identification techniques have been proposed (Nagarajaiah and Dharap, 2003; Nagarajaiah and Li, 2004)

Signal based identification, based on analysis of response signals of structures, has also been developed. The classical method of frequency domain analysis is by means of Fourier transform, and its algorithmic implementation, the Discrete Fourier Transformation (DFT). Though DFT has been widely used for modal analysis and other system identification tasks, it has several limitations. Fourier analysis is inherently global in nature and provides average information over time, ignoring the time varying nature of a nonstationary signal.

In parallel with the advances in sensing and data acquisition techniques, there has been a tremendous amount of development of signal processing techniques, which allows extraction of information from the available data sensed in the form of either signals or images. Several identification techniques have been proposed for structural dynamic systems in the recent past (Worden and Tomlinson, 2001). Most of the techniques and algorithms proposed are based on the use of different integral transforms. Among the available techniques, those based on the use of Hilbert transform (HT) by Tomlinson (1987) and Feldman (1994a,b) have become popular. Time-frequency methods (Cohen, 1995; Huang *et al.*, 1998), such as short-time Fourier transform (STFT) and wavelets, are used extensively for signal processing. New techniques such as Empirical Mode Decomposition (EMD) (Huang *et al.*, 1998) have been developed for signal processing of non-stationary signals. STFT and EMD techniques, with Hilbert Transform, have played a key role in the development of new time-frequency based controllers for semiactive, smart tuned mass dampers (Nagarajaiah *et al.*, 1999; Nagarajaiah and Varadarajan, 2001, 2005; Nagarajaiah and Sonmez, 2007; Nagarajaiah, 2009; Narasimhan and Nagarajaiah, 2005; Varadarajan and Nagarajaiah, 2004). Modal identification using EMD and HT has been developed

(Nagarajaiah and Varadarajan, 2001; Nagarajaiah, 2009; Yang *et al.*, 2003, 2004). Wavelets have played a key role in the development of new linear quadratic time varying controllers (Basu and Nagarajaiah, 2008) and modal identification of time varying systems (Basu *et al.*, 2008) by the authors. Wavelets, with HT, have also been used to estimate frequency and damping (Staszewski, 1997), modal and damage identification (Staszewski *et al.*, 1998; Staszewski and Robertson, 2007; Basu 2007; Chakraborty *et al.*, 2006; Basu and Nagarajaiah, 2008; Pakrashi *et al.*, 2007; Goggins *et al.*, 2006).

Recently, several time-frequency analysis tools, particularly the wavelet analysis technique, have proved to be powerful for system assessment, structural health monitoring and fault monitoring (Staszewski and Tomlinson, 1994; Wang and McFadden, 1996; Al-Khalidy *et al.*, 1997; Ghanem and Romeo, 2000; Addison *et al.*, 2002), system identification (Staszewski, 1997, 1998; Ruzzene *et al.*, 2000, Gurley and Kareem, 1999; Kitada, 1998; Kyprianou and Staszewski, 1999; Robertson *et al.*, 1998; Lardies and Gouttebroze, 2000; Piombo *et al.*, 2000; Ghanem and Romeo, 2001; Kijewski and Kareem 2003, 2006, 2007) and damage detection (Naldi and Venini, 1997; Staszewski *et al.*, 1998; Liew and Wang, 1998; Okafor and Dutta, 2000; Wang and Deng, 1999; Hou *et al.*, 2000; Patsias *et al.*, 2002; Melhem and Kim, 2003; Chang and Chen, 2003; Gentile and Messina, 2003; Loutridis *et al.*, 2004; Rucka and Wilde, 2006; Spanos *et al.*, 2006) by analysing vibration signals. Some of the early researchers on analysis of vibration signals using wavelets include (Newland, 1993; 1994a,1994b; Zeldin and Spanos, 1998; Basu and Gupta, 1997,1998,1999a,b). These references are representative of the vast amount of literature available as a result of research in the past decade and a half. An overview on wavelet analysis with several different applications has been provided by Robertson and Basu (2008) and Staszewski and Robertson (2007).

The primary objective of this paper is to develop output only modal identification and structural damage detection. Identification of multi-degree of freedom (MDOF) linear time invariant (LTI) and linear time variant (LTV—due to damage) systems based on Time-frequency (TF) techniques—such as short-time Fourier transform (STFT), empirical mode decomposition (EMD), and wavelets—is proposed. STFT, EMD, and wavelet methods developed to date are reviewed in sufficient detail. In addition, a Hilbert transform (HT) approach to determine frequency and damping is also presented. In this paper, STFT, EMD, HT and wavelet techniques are developed for decomposition of free vibration response of MDOF systems into their modal components. Once the modal components are obtained, each one is processed using Hilbert transform to obtain the modal frequency and damping ratios. In addition, the ratio of modal components at different degrees of freedom facilitate determination of mode shape. In cases

with output only modal identification using ambient/random response, the random decrement technique is used to obtain the free vibration response.

The advantage of TF techniques is that they are signal based; hence, can be used for output only modal identification. A three degree of freedom 1:10 scale model test structure is used to validate the proposed output only modal identification techniques based on STFT, EMD, HT, wavelets. Both measured free vibration and forced vibration (white noise) response are considered. The secondary objective of this paper is to show the relative ease with which the TF techniques can be used for modal identification and their potential for real world applications where output only identification is essential. Recorded ambient vibration data processed using techniques such as the random decrement technique can be used to obtain the free vibration response, so further processing using TF based modal identification can be performed.

2 Time-frequency methods: STFT, EMD, and HT

2.1 Analytical signal and Hilbert transform

Signals in nature are real valued but for analysis, it is often more convenient to deal with complex signals. One wants the real part, $s(t)$, of the complex signal, $s_a(t)$, to be the actual signal under consideration. How is the imaginary part, $\bar{s}(t)$, fixed to form the complex signal? In particular, to write a complex signal, how is $\bar{s}(t)$ chosen? the standard method is to form the "analytic" signal, $s_a(t)$,

$$s_a(t) = s(t) + j\bar{s}(t) \tag{1}$$

where $j = \sqrt{-1}$. This can be achieved by taking the spectrum of the actual signal, $s(\omega)$, deleting the negative part of the spectrum, retaining only the positive part of the spectrum, multiply it by a factor of 2, and then form the new (complex) signal by Fourier inversion. More specifically if there is a real signal, $s(t)$, calculate $s(\omega)$. Form the complex signal with the positive part of $s(\omega)$ only,

$$s_a(t) = 2\frac{1}{\sqrt{2\pi}}\int_0^\infty s(\omega)e^{j\omega t}d\omega \tag{2}$$

The factor of two is inserted so that the real part of the complex signal will be equal to the real signal one started out with. Therefore, substituting for $s(\omega)$

$$s_a(t) = \frac{1}{\pi}\int_0^\infty \int s(t')e^{-j\omega t'}e^{j\omega t}dt'd\omega \tag{3}$$

Using the fact that

$$\int_0^\infty e^{j\omega x}d\omega = \pi\delta(x) + \frac{j}{x} \tag{4}$$

Results in

$$\int_0^\infty e^{j\omega(t-t')}d\omega = \pi\delta(t-t') + \frac{j}{t-t'} \tag{5}$$

Hence

$$s_a(t) = \frac{1}{\pi}\int s(t')\left(\pi\delta(t-t') + \frac{j}{t-t'}\right)dt' \tag{6}$$

or

$$s_a(t) = s(t) + \frac{j}{\pi}\int_{-\infty}^\infty \frac{s(t')}{t-t'}dt' \tag{7}$$

The imaginary part turns out to be the Hilbert transform:

$$\bar{s} = H[s(t)] = \frac{1}{\pi}\int_{-\infty}^\infty \frac{s(t')}{t-t'}dt' \tag{8}$$

Hence,

$$s_a(t) = s(t) + jH[s(t)] = s(t) + j\bar{s} \tag{9}$$

The complex signal thus formed, $s_a(t)$, is called the analytic signal. Note that by definition analytic signals are signals whose spectrum consist only of positive frequencies. That is, the spectrum is zero for negative frequencies.

As per Eqs. (1) – (9), the analytic signal can be obtained by: (1) taking the Fourier transform of $s(t)$; (2) zeroing the amplitude for negative frequencies and doubling the amplitude for positive frequencies; and (3) taking the inverse Fourier transform. The analytic signal $s_a(t)$ can also be expressed as

$$s_a(t) = A(t)e^{j\varphi(t)} \tag{10}$$

where, $A(t)$ = instantaneous amplitude and $\varphi(t)$ = instantaneous phase

2.2 Instantaneous frequency

In the analytic signal given by Equation 1 and 10, $A(t) = \sqrt{s^2(t) + \bar{s}^2(t)}$ and $\varphi(t) = \arctan\left(\frac{\bar{s}(t)}{s(t)}\right)$, the instantaneous frequency $\omega_i(t)$ is given by

$$\omega_i(t) = \dot{\varphi}(t) = \frac{d}{dt}\left(\arctan\left(\frac{\bar{s}(t)}{s(t)}\right)\right) \tag{11}$$

where

$$\frac{d\varphi}{dt} = \frac{1}{1+\left(\frac{\bar{s}^2(t)}{s^2(t)}\right)^2}\frac{d}{dt}\left(\frac{\bar{s}(t)}{s(t)}\right) \tag{12}$$

and

$$\frac{d}{dt}\left(\frac{\bar{s}(t)}{s(t)}\right) = \frac{s(t)\dot{\bar{s}}(t) - \bar{s}(t)\dot{s}(t)}{s^2(t)} \tag{13}$$

From Eqs. (12) and (13) one gets

$$\omega_i(t) = \frac{\mathrm{d}\varphi(t)}{\mathrm{d}t} = \frac{(s(t)\overline{s}(t) - \overline{s}(t)\dot{s}(t))}{s^2(t) + \overline{s}^2(t)} \quad (14)$$

2.3 Short-time Fourier transform and spectrogram

The Fourier transform (FT) of a signal $s(t)$ is given by $s(\omega) = \frac{1}{\sqrt{2\pi}} \int s(t) \mathrm{e}^{-\mathrm{j}\omega t} \mathrm{d}t$. The short-time Fourier transform (STFT), the first tool devised for analyzing a signal in both time and frequency, is based on FT of a short portion of signal $s_h(\tau)$ sampled by a moving window $h(\tau\text{-}t)$. The running time is τ and the fixed time is t. Since the time interval is short compared to the whole signal, this process is called taking the STFT.

$$s_t(\omega) = \frac{1}{\sqrt{2\pi}} \int_{-\infty}^{\infty} s_h(\tau) \mathrm{e}^{-\mathrm{j}\omega\tau} \mathrm{d}\tau \quad (15)$$

where $s_h(\tau)$ is defined as follows:

$$s_h(\tau) = s(\tau)h(\tau - t) \quad (16)$$

in which $h(\tau\text{-}t)$ is an appropriately chosen window function that emphasizes the signal around the time t, and is a function $\tau\text{-}t$, i.e., $s_h(\tau) = s(\tau)$ for τ near t and $s_h(\tau) = 0$ for τ far away from t. Considering this signal as a function of τ, one can ask for the spectrum of it. Since the window has been chosen to emphasize the signal at t, the spectrum will emphasize the frequencies at that time and hence give an indication of the frequencies at that time. In particular, the spectrum is,

$$s_t(\omega) = \frac{1}{\sqrt{2\pi}} \int_{-\infty}^{\infty} s(\tau)h(\tau - t)\mathrm{e}^{-\mathrm{j}\omega\tau} \mathrm{d}\tau \quad (17)$$

which is the short-time Fourier transform (STFT).

Summarizing, the basic idea is that to find the frequency content of the signal at a particular time, t, take a small piece $s_h(\tau)$ of the signal around that time and Fourier analyze it, neglecting the rest of the signal, obtaining a spectrum at that time. Next, take another small piece, of equal length of the signal, at the next time instant and get another spectrum. Continue until the entire signal is sampled. The collection of all these spectrum (or slices at every time instant) gives a time-frequency spectrogram that covers the entire signal, and captures the localized time varying frequency content of the signal. If one performs a FT, then the localized variations of frequency content are lost, since FT is performed on the whole signal; the result is an average spectrum of all those obtained by STFT.

The energy density of the modified signal and the spectrogram is given by,

$$P(t,\omega) = \left| s_t(\omega) \right|^2 \quad (18)$$

or

$$P_{\mathrm{sp}}(t,\omega) = \left| \frac{1}{\sqrt{2\pi}} \int_{-\infty}^{\infty} s(\tau)h(\tau - t)\mathrm{e}^{-\mathrm{j}\omega\tau} \mathrm{d}\tau \right|^2 \quad (19)$$

By analogy with the previous discussion, it can be used to study the behavior of the signal around the frequency point ω. This is done by choosing a window function whose transform is weighted relatively higher at the frequency ω.

$$H(\omega) = \frac{1}{\sqrt{2\pi}} \int_{-\infty}^{\infty} h(t)\,\mathrm{e}^{-\mathrm{j}\omega t} \mathrm{d}t \quad (20)$$

$$s_{\omega}(t) = \frac{1}{\sqrt{2\pi}} \int_{-\infty}^{\infty} s(\omega')H(\omega - \omega')\mathrm{e}^{\mathrm{j}\omega' t} \mathrm{d}\omega' \quad (21)$$

$$s_h(\tau) = s(\tau)h(\tau - t) = \frac{1}{\sqrt{2\pi}} \int_{-\infty}^{\infty} s_t(\omega)\mathrm{e}^{\mathrm{j}\omega t} \mathrm{d}\omega \quad (22)$$

where ω' is running frequency and fixed frequency is ω. The spectrogram is given by

$$P_{\mathrm{sp}}(t,\omega) = \left| \frac{1}{\sqrt{2\pi}} \int_{-\infty}^{\infty} s(\omega')H(\omega - \omega')\mathrm{e}^{\mathrm{j}\omega' t} \mathrm{d}\omega' \right|^2 \quad (23)$$

The limitation of STFT is its fixed resolution (this is discussed in more detail in the section on wavelets), which can overcome multi-resolution analysis using wavelets. In STFT, the length of the signal segment chosen or the length of the windowing function $h(t)$ determines the resolution: broad window results in better frequency resolution but poor time resolution, and narrow window results in good time resolution but poor frequency resolution, due to the time-bandwidth relation (uncertainty principle (Cohen, 1995)). Note $h(t)$ and $H(\omega)$ are Fourier transform pairs (Eq.(20), i.e., if $h(t)$ is narrow, more time resolution is obtained, however, $H(\omega)$ becomes broad resulting in poor frequency resolution and vice versa.

2.4 STFT implementation procedure

The implementation procedure for the STFT in the discrete domain is carried out by extracting time windows of the original nonstationary signal $s(t)$. After zero padding and convolving the signal with Hamming window, the DFT is computed for each windowed signal to obtain STFT, $s_t(\omega)$, of signal $s_h(\tau)$. If the window width is $n.\Delta t$ (where n is number of points in the window, and Δt is the sampling rate of the signal), the k-th element in $s_t(\omega)$ is the Fourier coefficient that corresponds to the frequency,

$$\omega_k = \frac{2\pi k}{n\Delta t}\left(\text{for window width } n\Delta t \right) \quad (24)$$

2.5 Empirical mode decomposition

For a multicomponent signal–as in a multimodal or multi-degree of freedom (MDOF) response--the procedure described in the previous section to obtain analytic signal and instantaneous frequency cannot be applied directly, as described earlier. The empirical mode decomposition (EMD) technique, developed by Huang (1998), adaptively decomposes a signal into "intrinsic mode functions" which can then be converted to an analytical signal using HT. The time-frequency representation and instantaneous frequency can be obtained from the intrinsic modes extracted from the decomposition, using HT. The principle technique is to decompose a signal into a sum of functions that (1) have the same number of zero crossings and extrema, and (2) are symmetric with respect to the local mean. The first condition is similar to the narrow-band requirement for a stationary Gaussian process. The second condition modifies a global requirement to a local one, and is necessary to ensure that the instantaneous frequency will not have unwanted fluctuations as induced by asymmetric waveforms. These functions are called intrinsic mode functions (IMF denoted by imf_i) and are obtained iteratively (Huang *et al.*, 1998). The signal, $x_j(t)$, for example, jth degree of freedom displacement of a MDOF system, can be decomposed as follows

$$x_j(t) = \sum_{i=1}^{n} \text{imf}_i(t) + r_n(t) \qquad (25)$$

where $\text{imf}_i(t)$ are the "intrinsic mode functions" (note: dominant IMFs are equivalent to individual modal contributions to $x_j(t)$-which will be demonstrated in a later section) and $r_n(t)$ is the residue of the decomposition. The intrinsic mode functions are obtained using the following algorithm:

1. Initialize; $r_0 = x_j(t), i=1$
2. Extract the imf_i as follows:
(a) Initialize: $h_0(t) = r_{i-1}(t), j=1$
(b) Extract the local minima and maxima of $h_{j-1}(t)$
(c) Interpolate the local maxima and the local minima by a spline to form upper and lower envelopes of $h_{j-1}(t)$, $e_{\max}(t)$ and $e_{\min}(t)$ respectively.
(d) Calculate the mean m_{j-1} of the upper and lower envelopes $= (e_{\max}(t) + e_{\min}(t))/2$
(e) $h_j(t) = h_{j-1}(t) - m_{j-1}(t)$.
(f) If stopping criterion is satisfied then set $\text{imf}_i(t) = h_j(t)$ else go to (b) with $j = j+1$
3. $r_i(t) = r_{i-1}(t) - \text{imf}_i(t)$
4. If $r_i(t)$ still has at least 2 extrema then go to 2 with $i = i + 1$ else the decomposition is finished and $r_i(t)$ is the residue.

The analytical signal, $s_a(t)$, and the instantaneous frequencies $\omega_i(t)$, associated with each $\text{imf}_i(t)$ component can be obtained using Eqs. (1) - (14) by letting $s(t) = \text{imf}_i(t)$ and $s_a(t) = s(t) + jH(\overline{s(t)})$ for each

IMF component.

To ensure that the IMF components retain the amplitude and frequency modulations of the actual signal, a satisfactory stopping criteria for the sifting process is defined (Rilling *et al.*, 2003). A criteria for stopping is accomplished by limiting the standard deviation, SD (Huang *et al.*, 1998), of $h(t)$, obtained from consecutive sifting results as

$$\text{SD} = \sum_{k=0}^{l} \left[\frac{\left|\left(h_{j-1}(k\Delta t) - h_j(k\Delta t)\right)\right|^2}{h_{j-1}^2(k\Delta t)} \right] \qquad (26)$$

where $l = T/\Delta t$ and T = total time. A typical value for SD is set between 0.2 and 0.3 (Rilling *et al.*, 2003). An improvement over this criterion is based on two thresholds θ_1 and θ_2, aimed at globally small fluctuations in the mean while taking into account locally large excursions. This amounts to introducing a mode amplitude $a(t)$ and an evaluation function $\sigma(t)$:

$$a(t) = \left(\frac{e_{\max}(t) - e_{\min}(t)}{2} \right) \qquad (27)$$

$$\sigma(t) = \left| \frac{m(t)}{a(t)} \right| \qquad (28)$$

Sifting is iterated until $\sigma(t) < \theta_1$ for a fraction of the total duration while $\sigma(t) < \theta_2$ for the remaining fraction. Typically $\theta_1 \approx 0.05$ and $\theta_2 \approx 10\theta_1$ (Rilling *et al.*, 2003).

3 Modal identification of LTI and LTV systems using EMD/HT and STFT

EMD can be used to decompose a signal into its multimodal components (+ residual IMF components + residue). In a lightly damped system with distinct modes, EMD can extract the multicomponent modal contributions [or IMFs] from the j th DOF displacement response of a MDOF system. Each of these IMF components can then be analyzed separately to obtain the instantaneous frequency and damping ratios. If the displacement of MDOF LTI system is represented by vector $\boldsymbol{x} = \boldsymbol{\Phi q}$, where $\boldsymbol{\Phi}$ = modal matrix, $\boldsymbol{q}$ = modal displacement vector, then combining it with equation 25 leads to the following equation for $x_j(t)$, the jth degree of freedom displacement of a MDOF LTI system,

$$x_j(t) = \sum_{i=1}^{n} \text{imf}_i(t) + r_n(t) = \sum_{i=1}^{m} \boldsymbol{\Phi}_{ji} q_i(t) + \sum_{i=m}^{n} \text{imf}_i(t) + r_n(t) \qquad (29)$$

where m = number of modes of a MDOF system and

IMF's from m to n are treated as residual terms along with the actual residual and discarded.

The equation of motion of a MDOF is given by

$$M\ddot{x} + C\dot{x} + Kx = MRf \tag{30}$$

substituting $x = \Phi q$,

$$\Phi^T M\Phi\ddot{q} + \Phi^T C\Phi\dot{q} + \Phi^T K\Phi q = \Phi^T MRf \tag{31}$$

A proportionally damped system with orthonormal Φ leads to m uncoupled equations of motion with

$$\mathrm{diag}[\Lambda_c] = \begin{bmatrix} 2\xi_1\omega_1 & 0 & \cdot & \cdot & \cdot & 0 \\ 0 & 2\xi_2\omega_2 & \cdot & \cdot & \cdot & 0 \\ \cdot & \cdot & \cdot & \cdot & \cdot & \cdot \\ \cdot & \cdot & \cdot & \cdot & \cdot & \cdot \\ \cdot & \cdot & \cdot & \cdot & \cdot & \cdot \\ 0 & 0 & 0 & 0 & 0 & 2\xi_n\omega_n \end{bmatrix}$$

$$\mathrm{diag}[\Lambda_k] = \begin{bmatrix} \omega_1^2 & 0 & \cdot & \cdot & \cdot & 0 \\ 0 & \omega_2^2 & \cdot & \cdot & \cdot & 0 \\ \cdot & \cdot & \cdot & \cdot & \cdot & \cdot \\ \cdot & \cdot & \cdot & \cdot & \cdot & \cdot \\ \cdot & \cdot & \cdot & \cdot & \cdot & \cdot \\ 0 & 0 & 0 & 0 & 0 & \omega_n^2 \end{bmatrix}$$

$$\ddot{q}_k + 2\xi_k\omega_k\dot{q}_k + \omega_k^2 q_k = \Gamma_k f \tag{32}$$

where $\Gamma_k = \Phi_k^T MR$. With f as input and q_k as output, taking Laplace transform

$$\left(s^2 + 2\xi_k\omega_k s + \omega_k^2\right)q_k(s) = \Gamma_k f(s) \tag{33}$$

Dropping Γ_k for generality, the transfer function is then given by

$$H_k(s) = \frac{1}{s^2 + 2\xi_k\omega_k s + \omega_k^2} \tag{34}$$

and the frequency response function (FRF) is given by

$$H_k(j\omega) = \frac{1}{-\omega^2 + j2\xi_k\omega_k\omega + \omega_k^2} \tag{35}$$

Noting $x_k = \Phi_k q_k$ and x_{jk} as the jth component of the displacement contributed by the kth mode, and with f as input and x_{jk} as output, the transfer function

$$H_{jk}(j\omega) = \frac{1}{\left(\omega_k^2 - \omega^2\right) + j2\xi_k\omega_k\omega}\phi_{jk} \tag{36}$$

If the structure is lightly damped, the peak transfer function occurs at $\omega = \omega_k$ with amplitude

$$\left|H_{jk}(j\omega)\right| = \frac{\sqrt{1 + 4\xi_k^2}}{2\xi_k}\phi_{jk} \tag{37}$$

From Eq. (37) it is seen that magnitudes of the peaks of FRF at $\omega = \omega_k$ are proportional to the components of the kth modal vector. The sign of these components can be determined by phases associated with the FRF's: if two modal components are in phase, they are of the same sign and if the two modal components are out-of-phase, they are of opposite sign. With the knowledge of magnitude of peaks, the damping factor, ξ_k can be solved from Eq. (37). From Eq. (36), summing over all modes gives

$$H_{ij}(j\omega) = \sum_{k=1}^{n}\frac{\phi_{ik}\phi_{jk}}{\left(\omega_k^2 - \omega^2\right) + j2\xi_k\omega_k\omega} \tag{38}$$

which can be written as

$$H_{ij}(j\omega) = \sum_{k=1}^{n}\frac{{}_k A_{ij}}{\left(\omega_k^2 - \omega^2\right) + j2\xi_k\omega_k\omega} \tag{39}$$

where ${}_k A_{ij} = \phi_{ik}\phi_{jk}$ being the residues or modal components. Taking the inverse transform of Eq. (39) gives the general form of the impulse response function (IRF)

$$h_{ij}(t) = \sum_{k=1}^{n}\frac{{}_k A_{ij}}{\omega_{dk}}e^{-\xi_k\omega_k t}\sin\left(\omega_{dk}t\right) \tag{40}$$

where $\omega_{dk} = \omega_k\sqrt{1 - \xi_k^2} =$ damped frequency of the kth mode. It follows from Eq. (39) that MDOF linear time invariant system frequency responses are the sum of n single degree of freedom frequency responses, provided that well separated modes and light proportional damping are valid, and the residues and the modes are real. For non-proportionally damped systems, the residues and modes become complex.

Consider the function $e^{-\sigma_k + j\omega_k t}$ with $\sigma_k = \xi_k\omega_{nk}$ and $\omega_k = \omega_{dk}$, and for a damped asymptotically stable system with $\sigma > 0$, Eq. (36) for mode k can be rewritten by taking the inverse Fourier transform

$$h_{jk}(t) = A_{jk}e^{-\sigma_k t}\sin\left(\omega_{dk}t\right) \tag{41}$$

$$\bar{h}_{jk}(t) = A_{jk}e^{-\sigma_k t}\cos\left(\omega_{dk}t\right) \tag{42}$$

where $A_{jk} = \dfrac{\phi_{jk}}{\omega_{dk}}$ leading to the analytical signal

$$h_{jk_a}(t) = h_{jk}(t) + j\bar{h}_{jk}(t) \tag{43}$$

that can be written as

$$h_{jk_a}(t) = \bar{A}_{jk}e^{j\varphi t} \tag{44}$$

The magnitude of this analytical signal is given by

$$\left| h_{jk_a}(t) \right| = \left| \overline{A}_{jk} \right| = \sqrt{h_{jk_a}^2(t) + \overline{h}_{jk_a}^2(t)} \qquad (45)$$

Substituting Eq. (3) and simplifying the results in

$$\left| \overline{A}_{jk} \right| = A_{jk} e^{-\sigma_k t} \qquad (46)$$

Taking the natural logarithm of this expression yields

$$\log \left| \overline{A}_{jk} \right| = -\sigma_k t + \log(A_{jk}) = -\xi_k \omega_n t + \log(A_{jk}) \qquad (47)$$

3.1 Modal identification based on empirical mode decomposition

Nagarajaiah and coworkers originally developed the EMD/HT modal identification approach for tuning STMD in 2001 (Nagarajaiah and Varadarajan, 2001), based on their earlier work (Nagarajaiah *et al.*, 1999) on variable stiffness systems. The advantage of this approach is that it is signal based and output only; hence, measured response at any one DOF can be used to make useful estimates of instantaneous frequency and damping ratio. However, the capability to estimate mode shape response signals at more degrees of freedom will be needed. Each significant IMF component represents one modal component with unique instantaneous frequency and damping ratio.

Individual mode FRF and corresponding IRF can be extracted when band pass filters (Thrane, 1984) are applied to the system FRF. Equation (46) can be used to estimate damping in the *k*th mode, as suggested originally by Thrane in 1984 and adopted by Agneni in 1989. In 2003, Yang and coworkers (Yang *et al.*, 2003, 2004) extended this approach by using EMD/HT to decompose and obtain IMFs and perform modal identification. In cases, when the inputs are white noise excitation and the output accelerations at a certain floor are available, the free vibration response from the stationary response to white noise can be obtained using the random decrement technique (Ibrahim, 1977) followed by instantaneous frequency and damping calculations.

The EMD/HT outlined below was developed independently by Nagarajaiah and coworkers (Nagarajaiah and Varadarajan, 2001):

(1) Obtain signal $x_j(t)$, *j*th degree of freedom displacement of a MDOF system, from the feedback response.

(2) Decompose the signal $x_j(t)$ into its IMF components as described in Eqs. (29) and (25).

(3) Construct the analytical signal for each IMF/modal component using Hilbert transform method described in Eq. (9).

(4) Obtain the phase angle of the analytic signal and then obtain the instantaneous frequency from Eq. (14).

(5) Obtain the log amplitude function of the analytic signal; perform least squares line fit to the function (which will be a decreasing function fluctuating about a line and not necessarily linear at all times). Then, using Eq. (47), compute the slope and damping ratio.

(6) The ratio of modal components at different degrees of freedom facilitate determination of mode shape.

(7) In cases of output only modal identification with ambient/random excitation, use the random decrement technique (Ibrahim, 1977) to obtain free vibration response.

3.2 Modal identification based on STFT

After obtaining a spectrogram, a FRF at a given time can be extracted, and the individual mode FRF and corresponding IRF can be extracted when band pass filters (Thrane, 1984) are applied. The frequencies can be identified by applying HT to the IRF as per Eq. (44). Equation (46) can be used to estimate damping in the *k*th mode, as suggested originally by Thrane in 1984 and adopted by Agneni in 1989. The ratio of modal components at different degrees of freedom facilitate determination of mode shape. In cases of output only modal identification with ambient/random excitation, the random decrement technique can be used to obtain the free vibration response.

4 Modal identification of lTI and lTY systems using wavelets

The wavelet function can be defined as

$$(W_\psi x)(a,b) = \frac{1}{\sqrt{a}} \int_{-\infty}^{\infty} x(t) \psi^* \left(\frac{t-b}{a} \right) dt \qquad (48)$$

where *b* is a translation indicating the locality, *a* is a dilation or scale parameter, $\psi(t)$ is an analyzing (basic) wavelet and $\psi^*(\cdot)$ is the complex conjugate of $\psi(\cdot)$. Each value of the wavelet transform $(W_\psi x)(a,b)$ is normalized by the factor $1/\sqrt{a}$. This normalization ensures that the integral energy given by each wavelet $\psi_{a,b}(t)$ is independent of the dilation *a*. The function $\psi(t)$ qualifies for an analyzing wavelet, when it satisfies the admissibility condition

$$C_\psi = \int_{-\infty}^{\infty} \left(\frac{|\psi(\omega)|^2}{|\omega|} \right) d\omega < \infty \qquad (49)$$

where $\psi(\omega)$ is the fourier transform of $\psi(t)$. This is necessary for obtaining the inverse of the wavelet transform given by

$$x(t) = \frac{1}{C_\psi} \int_{-\infty}^{\infty} \int_{-\infty}^{\infty} (W_\psi x)(a,b) \frac{1}{\sqrt{a}} \psi^* \left(\frac{t-b}{a} \right) \frac{da\,db}{a^2} \qquad (50)$$

The possibility of time-frequency localization arises from the $\psi(t)$ being a window function, which means that additionally

$$\int_{-\infty}^{\infty} |\psi(t)| \mathrm{d}t < \infty \qquad (51)$$

which follows from Eq. (45). One of the most widely used functions in wavelet analysis is the Morlet wavelet defined by

$$\psi(t) = \mathrm{e}^{\mathrm{j}2\pi f_0 |t|} \mathrm{e}^{\frac{-|t|^2}{2}} \qquad (52)$$

The Fourier spectrum of Morlet wavelet is a shifted Gaussian function

$$\widehat{\psi}(f) = \sqrt{2}\pi \mathrm{e}^{-2\pi^2 (f-f_0)^2} \qquad (53)$$

In practice, the value of $f_0 > 5$ is used. The wavelet transform is a linear representation of a signal. Thus it follows that for a given N functions x_i and N complex values $a_i (i = 1, 2, \cdots, N)$

$$\left(W_\psi \sum_{i=1}^{n} a_i x_i\right)(a,b) = \sum_{i=1}^{n} a_i (W_g x_i)(a,b) \qquad (54)$$

The frequency localization is clearly seen when the wavelet transform is expressed in terms of the Fourier transform,

$$(W_\psi x)(a,b) = \sqrt{a} \int_{-\infty}^{+\infty} X(f) \psi_{a,b}^*(af) \mathrm{e}^{\mathrm{j}2\pi fb} \mathrm{d}f \qquad (55)$$

where $\psi^*(\cdot)$ is the complex cojugate of $\psi(\cdot)$. This localization depends on the dilation parameter a. The local resolution of the wavelet transform in time and frequency is determined by duration and bandwidth of the analyzing functions given by

$$\Delta t = a \Delta t_\psi, \Delta f = \Delta f_\psi / a \qquad (56)$$

where Δt_ψ and Δf_ψ are duration and bandwidth of the basic wavelet function, respectively. For the Morlet analyzing wavelet function, the relationship between the dilation parameter a_f and the signal frequency f_x at which the analyzing wavelet function is focused, can be given as

$$a_f = f_0 \left(\frac{f_s}{f_w}\right)\left(\frac{1}{f_x}\right) \qquad (57)$$

where f_s and f_w are the sampling frequencies of the signal and the analyzing wavelet, respectively. The frequency bandwidth of the wavelet function for the given dilation a can be obtained using a frequency representation of the Morlet wavelet and expressed as

$$\Delta f_x = \left(\frac{1}{\pi a}\right)\left(\frac{f_s}{f_w}\right) \qquad (58)$$

this allows one to obtain a single element of the wavelet decomposition of the function for a given value of frequency (dilation) and frequency bandwidth.

The wavelets are scaled to obtain a range of frequencies. They are also translated to provide the time information in the transform. The wavelet transform works as a filter, allowing only a certain time and frequency content through. Any given atom in the time-frequency map of the wavelet transform (see Fig. 1) represents the correlation between the wavelet basis function at that frequency dilation and the signal in that time segment. The frequency content of the wavelet transform is represented in terms of scales, which are inversely related to frequencies. The squared amplitude of the continuous wavelet transform (CWT) is therefore called the scalogram. The relationship between scales and frequencies can be used to form a time-frequency map from the scalogram.

Since the wavelet works in a manner similar to the STFT, by convolving the signal with a function that varies in both time and frequency, it suffers from similar limitations in the resolution of the time-frequency map. Both transforms are confined by the uncertainty principle, which limits the area of a time-frequency atom in the overall time-frequency map (see Fig. 1). The biggest difference between the two transforms is that the
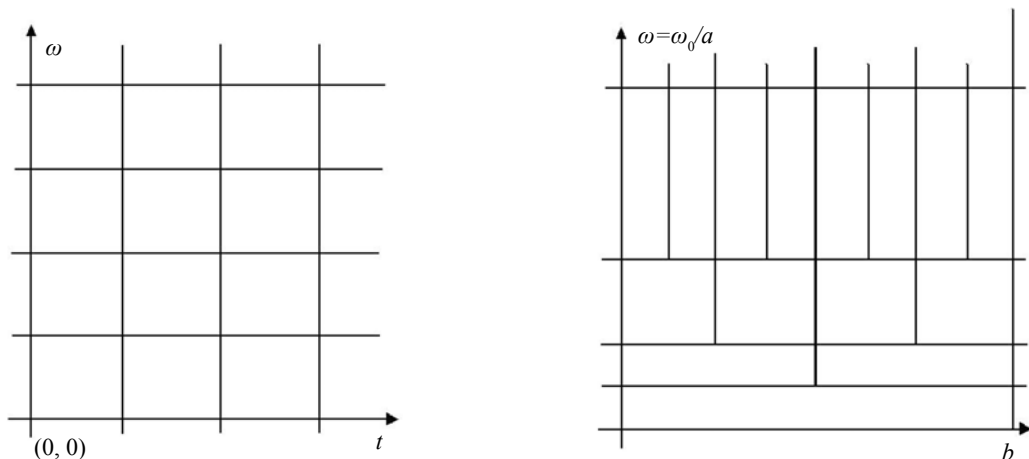

Fig. 1 Comparing STFT and wavelet transform resolution in time and frequency domain

atoms in the WT map are not a constant shape. In the lower frequencies, the atoms are fatter, providing a better resolution in frequency and worse resolution in time, whereas in the upper frequencies the atoms are taller, providing better time resolution and worse frequency resolution. This variable resolution can be advantageous in the analysis of structural time response data.

The continuous wavelet transform gets its name from the fact that the Mother wavelet is continuously shifted across the length of the data being analyzed. This smooth shifting means that the time/frequency atoms shown in Fig. 1 will overlap one another, providing redundant information.

The variable windowing feature of wavelet analysis leads to an important property exhibiting constant Q factor (defined as the ratio of the center frequency to bandwidth) analysis. For STFT, at an analyzing frequency ω_0, changing the window width will increase or decrease the number of cycles of ω_0 inside the window. In the case of wavelet transforms, with the change in window width, mean dilation or compression of the wavelet function changes. Hence, the carrier frequency becomes ω_0/a, for a window width changing from T to aT. However, the number of cycles inside the window remains constant.

The frequency resolution is proportional to the window width both in the case of STFT and wavelet transform. However, for wavelet transform, a center frequency shift necessarily accompanies a window width change (time scaling). Thus, Q-factor is invariant with respect to wavelet dilation and these dilated wavelets may be considered as constant-Q bandpass filters giving rise to the frequency selectivity of the CWT.

Since the wavelet transform is an alternative representation of a signal, it should retain the characteristics of the signal including the energy content in the signal. Thus, there should exist a similar relation to the Parseval's theorem which provides the energy relationship in the Fourier domain. The total energy of a signal in wavelet domain representation is:

$$E_f = \frac{1}{c_\psi} \int_{-\infty}^{\infty} \int_{-\infty}^{\infty} |WT(u,s)|^2 \frac{\mathrm{d}s\mathrm{d}u}{s^2} \qquad (59)$$

where, C_ψ is a scalar constant related to the Fourier transform of the wavelet basis (called 'admissibility constant'). The wavelet basis functions can be normalized in a way such that it can attain a value of unity. The differential energy of the signal in the differential tile of scale-translation plane in wavelet domain is $|WT(u,s)|^2 \frac{\mathrm{d}s\mathrm{d}u}{s^2}$ which leads to the construction of the scalogram.

4.1 Estimates of modal parameters in MDOF systems

Since the analyzing wavelet function has compact

support in the time and frequency domains, multi-component signals can be written as

$$(W_\psi x \sum_{i=1}^{N} x_i)(a,b) = \frac{1}{\sqrt{a}} \sum_{i=1}^{N} \int_{t-a\Delta t_\psi}^{t+a\Delta t_\psi} x(t)\psi^*(\frac{t-b}{a})dt \quad (60)$$

The response of an underdamped SDOF system can be expressed in the form

$$x(t) = A(t)\mathrm{e}^{\pm jw_n\sqrt{1-\xi^2}t} \qquad (61)$$

Assuming the envelope $A(t)$ is slowly varying, it follows (Staszewski, 1997; Chakraborty *et al.*, 2006)

$$\ln|W_\psi x(a,b)| \approx -\xi w_n b + \ln(A_0 |\psi^*(\pm a_0 jw_n\sqrt{1-\xi^2})|) \qquad (62)$$

Subsequently, the response of the MDOF system can be obtained as

$$\left|(W_\psi x \sum_{i=1}^{N} x_i)(a,b)\right| \approx \sum_{i=1}^{N} A_i \mathrm{e}^{-\xi_i w_{n_i} b} \left|\psi^*(\pm ja_i w_{n_i}\sqrt{1-\xi_i^2})\right| \quad (63)$$

Due to the compact support of the analyzing wavelet functions in time and frequency, the wavelet transform of each separate mode $i = 1, 2, \cdots, N$ becomes (Staszewski, 1997; Chakraborty *et al.*, 2006)

$$\left|(W_\psi x_i)(a,b)\right| \approx A(b)\mathrm{e}^{-\xi_i w_{n_i} b} \left|\psi^*(\pm ja_i w_{n_i}\sqrt{1-\xi_i^2})\right| \qquad (64)$$

For the given value of dilation a_i related to the natural frequency f_{n_i} of the system, the modulus of the wavelet transform plotted in a semi-logarithmic scale leads to

$$\ln\left|(W_\psi x_i)(a_i,b)\right| \approx -\xi_i w_{n_i} b + \ln(A_i |\psi^*(\pm a_i jw_{n_i}\sqrt{1-\xi_i^2})|) \qquad (65)$$

and forms the basis of identifying the damping.

The derivations so far are general and are applicable to any continuous wavelet basis with desired or suitable time-frequency characteristics. The next subsection provides the details of a wavelet basis used for identifying the modal parameters of an MDOF system.

4.2 Modified littlewood-paley (L-P) basis

An equivalent of the Harmonic wavelet, when the basis function is real, is the Littlewood-Paley wavelet. This wavelet basis function is defined by

$$\psi(t) = \frac{1}{2\pi} \frac{\sin(4\pi t) - \sin(2\pi t)}{t} \qquad (66)$$

A possible variation of the wavelet is one which retains the characteristics of the basis function (close to transient vibration signals, i.e., oscillatory and decaying) but could reduce the frequency bandwidth of the mother

wavelet. Hence, the derived modified wavelet is called the modified L-P wavelet and has been proposed and used by Basu and Gupta (1999a, b). The shifted and scaled version of this is called the baby modified L-P wavelets. This wavelet basis has also been used by Basu (2005, 2007) for damage detection in structures.

The modified L-P basis function is defined by

$$\psi(t) = \frac{1}{\pi\sqrt{\sigma-1}} \frac{\sin(\sigma\pi t) - \sin(\pi t)}{t} \qquad (67)$$

where σ (is a scalar) >1. In the frequency domain, the wavelet basis can be represented by

$$\widehat{\psi}(t) = \begin{cases} \dfrac{1}{\sqrt{2\pi(\sigma-1)}} & \text{for } \pi \le |\omega| \le \sigma\pi \\ 0 & \text{elsewhere} \end{cases}$$

By choosing appropriate values for the bandwidth, the frequency content of the mother wavelet can be adjusted. If for numerical computation the scaling parameter is discretized as $a_j = \sigma^j$ (in an exponential scale), then the scaled version of the mother basis function has mutually non-overlapping frequency bands and is also orthogonal. This property can be conveniently utilized to detect natural frequencies and modal properties for the dynamical systems as seen in the following sections.

4.3 Wavelet packets

While the constant Q-factor and coarser frequency resolution at high frequencies make the wavelet analysis computationally efficient, this may be a disadvantage for analysis of some signals for system/modal identification and structural health monitoring. Better resolution at high frequencies can be obtained by wavelet packet construction.

The discrete wavelet transform based on multi-resolution analysis (MRA) splits the signal into two bands, a higher band (by using a high pass filter) and a lower band (by using a low pass filter). The lower band is subsequently again split in two bands. This concept can be generalized by splitting the signal into several bands each time. In addition, there could be further splitting of the higher bands too, not just the lower band. This generalization of MRA produces outputs called wavelet packets. This is a deviation from constant-Q analysis and achieves the desired frequency resolution at high frequency bands. Wavelet packets through arbitrary band splitting can choose the most suitable resolution to represent a signal.

The resolution of signals with wavelet packets is not only possible using MRA based frequency filters in the time domain (starting with Haar wavelets) but also in the frequency domain. For the arbitrary resolution using frequency domain based filters, the construction

for wavelet packets should be based on a modified Littlewood-Paley (L-P) wavelet basis. The application of wavelet packets is particularly useful in system identification and damage detection for SHM, where finer resolution at higher frequency is desired.

4.4 Identification of modal parameters

To detect the bands of frequencies in which the natural frequencies lie, the energy corresponding to each band is calculated for a particular state of response using equation 59. The bands, which do not contain the natural frequencies, lead to insignificant energy contribution. Hence, the first 'n' bands with significant energy content are the bands where the natural frequencies are located. These bands are in increasing order corresponding to the first 'n' natural frequencies, i.e., the lowest frequency band has the first natural frequency and so on.

However, the chosen bands may lead to bands with relatively broad intervals in which the natural frequencies lie. To refine the estimates into finer intervals, so that natural frequencies can be determined to a better precision, wavelet packets are used. This is an extension of wavelet transform to provide level by level time- frequency description and is easily adaptable for the modified L-P basis. The wavelet packet enables extraction of information from signals with an arbitrary time-frequency resolution satisfying the product constraint in the time-frequency window. In this technique, to refine the estimation of the kth natural frequency, ω_{n_k}, located in the j_kth band, i.e., with frequency band $\left[\pi/a_{jk}, \sigma\pi/a_{jk}\right]$, further re-division is carried out. If it is required to further subdivide the band in 'M' parts, then again an exponential scale is used to divide the band so that the corresponding time domain function forms a wavelet basis function. In this approach (also sometimes, termed as sub-band coding), for theth band, the mother basis for the packet, $\psi^s(t)$ is formed with the frequency domain description

$$\widehat{\psi^s}(\omega) = \begin{cases} \dfrac{1}{\sqrt{2\pi(\delta-1)}} & \text{for } \pi \le |\omega| \le \delta\pi \\ 0 & \text{elsewhere} \end{cases}$$

where $\delta^M = \sigma$ [with σ (a scalar) >1]. The corresponding time domain description is given by

$$\psi^s(t) = \frac{1}{\sqrt{\pi(\delta-1)}} \frac{\sin(\delta\pi t) - \sin(\pi t)}{t} \qquad (68)$$

The frequency band for the pth sub-band within the original j_kth band is the interval $[\delta^{p-1}\pi/a_{jk}, \delta^p\pi/a_{jk}]$. The basis function for this is denoted by $\psi^{sp}_{a_{jk},b}(t)$. The wavelet coefficient in this sub-band is denoted by $W_{\psi sp}x_m(a_{jk}, b)$. Using the wavelet coefficients in these sub-bands and then applying similar expression as in Eq. (59) to estimate the relative energies in the sub-bands, the

natural frequencies can be obtained more precisely.

Once the natural frequencies are obtained and the corresponding bands are identified, the following expression corresponding to the sub-band containing the kth natural frequency with scale parameter j_k and the sub-band parameter 'p' is considered to obtain the kth mode shape.

$$W_\psi x_i(a_j,b) = \sum_{k=1}^{N} \Phi_i^k W_\psi(a_{jk},b); i=1,2,\cdots,N \qquad (69)$$

Considering the response or two states or DOF in a MDOF system, (with one arbitrarily chosen as $i = 1$, without loss of generality), the ratio of wavelet coefficients of the two considered degrees of freedom at any instant of time $t = b$, corresponding to band j_k

$$\prod_{m}^{jk} = \frac{W_\psi x_i(a_{jk},b)}{W_\psi x_1(a_{jk},b)} = \frac{\Phi_m^k}{\Phi_1^k} \qquad (70)$$

Thus it is seen that the computed ratio of the wavelet coefficients are invariant with "b". These ratios for different states corresponding to different values of "m" and assuming $\Phi_1^j = 1$ (without loss of generality), the mode shape for the kth mode (in j_k band with further sub-band division) can be obtained as

$$\Phi_m^k = \prod_{m}^{jk}, \ m=1,2,\cdots,N \qquad (71)$$

4.5 Wavelet based online monitoring of LTV systems with stiffness changes

Consider a linear time varying multi-degree-of-freedom (MDOF) system with m degrees of freedom represented by the set of linear time varying ordinary differential equations with M, $C(t)$ and $K(t)$ as the mass, time varying damping and time varying stiffness matrices, respectively. The displacement response vector is denoted by $X(t) = \{x_1(t)x_2(t)\cdots x_m(t)\}^T$. Let us assume that the functions $K_{ij}(t); i,j=1\cdots m$ in the stiffness matrix have discontinuities at a finite number of points. It is then possible to divide the time in several segments with indices arranged as $t_0 < t_1 < t_2 < \cdots < t_n$ such that all $K_{ij}(t); i,j=1\cdots m$ are continuous functions in $[t_{i-1},t_i]$. Further, it is assumed that the variation of all the time varying stiffness functions are $K_{ij}(t)$ slower than the fundamental (lowest) frequency of the system (corresponding to the longest period). It subsequently follows that the variation of $X(t)$ may be represented with a slowly varying amplitude Φ_m^k and a slowly varying frequency $\omega_{ki}(t)$ at the kth mode, in the time interval $[t_{i-1},t_i]$.

The modified L–P function has been used as the wavelet basis for analysis for this problem and the basis is characterized by the Fourier transform

$$\widehat{\psi}(t) = \begin{cases} \dfrac{1}{\sqrt{F_1(\sigma-1)}} & \text{for } F_1 \le |\omega| \le \sigma F_1 \\ 0 & \text{otherwise} \end{cases}$$

where, F_1 is the initial cut off frequency of the mother wavelet. If this modified L–P basis function is used, then $\widehat{\psi}(a_j\omega)$ is supported over $\left[\sigma F_1/a_j, F_1/a_j\right]$. It follows that if $\omega_{k_i}(b)$ corresponding to the kth mode is in the j_kth band, i.e., $\omega_{k_i}(b) \in \left[F_1/a_j, F_1/a_{jk}\right]$, then it can be approximated as

$$\omega_{k_i}(b) \approx \omega_{0_{jk}} = \frac{\sigma+1}{2} \cdot \frac{\pi}{a_{jk}} \qquad (72)$$

for a lightly damped system (with $\eta_k = 1$), where $\omega_{0_{jk}}$ is the central frequency of the j_kth band. Let the parameters, $\omega_{1_i}(b), \omega_{2_i}(b),\ldots \omega_{m_i}(b)$, be contained in the bands with scale parameters identified by indices, respectively. Since, the response, $z_k(t)$ in the kth mode, i.e., in j_kth band is narrow banded with frequency around $\left[F_1/a_j, F_1/a_{jk}\right]$, it follows that the bands not containing the natural frequency have insignificant energy which leads to the approximation

$$\left|W_{\psi j}z_k(a_j,b)\right| \approx 0 \quad \text{if} \ \ j \ne j_k; \ k=1,2\cdots,m \qquad (73)$$

Thus, the 'm' bands with the 'm' natural frequency parameters $\omega^{ki}(b); k=1,2\cdots,m$ correspond to m local maxima in the variation of temporal energy, $E_j x_r(b)$ [or its proportional quantity $(1/a_j)\int_{b-\varepsilon}^{b+\varepsilon} \left|W_{\psi j}x_r(b)\right|^2 \mathrm{d}b$] (with the integral over $b-\varepsilon$ to $b+\varepsilon$ for the windowed data in case of online identification) with different values of the band parameter 'j'. It may be noted that since the wavelet basis is localized in time, the integral over the window is acceptable with the parameter ε is dependent on the frequency scale corresponding to j. If the forcing function is assumed to be described by a broad banded excitation, then by calculating the relative energies in different bands and comparing, it may be concluded that

$$E_{j-1}x_r(b) < E_j x_r(b) > E_{j+1}x_r(b); \quad \forall j = j_k; \quad k=1,2,\cdots,m \qquad (74)$$

if the modes are not too closely spaced. Once these bands are detected, the parameters $\omega_{k_i}(b)$ can be obtained as

$$\omega_{k_i}(b) \approx \frac{\sigma+1}{2} \cdot \frac{F_1}{a_{jk}}; \quad k=1,2,\cdots,m \qquad (75)$$

over the interval $[b-\varepsilon,b+\varepsilon]$. The sub-band coding with wavelet packets could be applied if the parameters $\omega_{k_i}(b)$ are desired to be obtained with better precision. Once the bands corresponding to the 'm' modes with the parameters $\omega_{k_i}(b)$ are obtained, the time varying

mode shapes $\{\boldsymbol{\Phi}(t)\}_j^k$ can be found by considering the wavelet coefficients of $x_r(t)$ with the scale parameters, j_k and sub-band parameter p (for wavelet packets). Now, considering two different states of response of the MDOF system with one considered as $r = 1$ (without the loss of generality), the ratio of wavelet coefficients of the considered states at the time instant $t = b$, gives the rth component of the time varying kth mode as

$$\pi_r^{jk}(b) = \frac{W_{\psi_{sp}} x_r(a_{jk}, b)}{W_{\psi_{sp}} x_1(a_{jk}, b)} = \frac{\Phi_j^k(b)}{\Phi_1^k(b)} \qquad (76)$$

5 Experimental and numerical validation of modal identification of LTI and LTV systems using STFT, EMD, wavelets and HT

5.1 Modal identification of 1:10 scale three story model using free vibration test results and STFT

The 1:10 scale three story model with a total weight of 1000 lbs, shown in Fig. 2, is used for the modal identification study based on the proposed STFT and EMD/HT algorithm. Time axis is scaled by from the prototype scale for this study. Measured third floor free vibration displacement response, shown in Fig. 2, is used for output only modal identification. Tests were also performed with white noise excitation and the FRF was estimated—for further details refer to Nagarajaiah (2009). The identified frequencies of the 3DOF structure, both from free vibration (output only) as well as forced vibration tests (input-output), are 5.5 Hz, 18.7 Hz, and 34 Hz for the three modes, respectively. The identified damping ratios are approximately 1.9%, 1.7% and 1.1% in the three modes, respectively, as shown in Table 1. At the prototype scale, the three modal frequencies are 1.75 Hz, 5.9 Hz and 10.7 Hz, respectively.

STFT is applied to the free vibration displacement response of the three story scaled building model. Figure 3 shows the time history (lower right), frequency spectrum (upper left), and the time-frequency spectrogram (upper right). The evolution of the frequency content of the displacement signal as a function of time can be seen in the spectrogram or time-frequency distribution (upper right), shown in Fig. 3. If one examines the time history alone (lower right) the

localized nature of the time varying frequency content is not evident. The modal free vibration response in the three separate modes and the time localization for each mode is clearly evident in the spectrogram, but not in the frequency spectrum or the time history—when examined independently. The three modal frequencies 5.5 Hz, 18.7 Hz and 34 Hz (Nagarajaiah, 2009) are clearly evident in the spectrogram and the frequency spectrum (upper left) shown in Fig. 3. After the STFT spectrogram reveals the modal frequencies, further processing is essential using band-pass filtering to obtain modal components as described in Section 3.2. Next, the EMD/HT and wavelet/HT based methods are presented which can accomplish output only modal identification without the use of band-pass filters.

5.2 Validation of EMD/HT technique using three story model free vibration test results

The three story scaled model, with the first mode frequency of 5.5 Hz, is subjected to free vibration tests. The measured third floor free vibration acceleration response signal (we use the acceleration signal since the third mode is dominant, while in the displacement signal it is not dominant) is then analyzed using EMD/HT to extract instantaneous frequency and damping ratios of
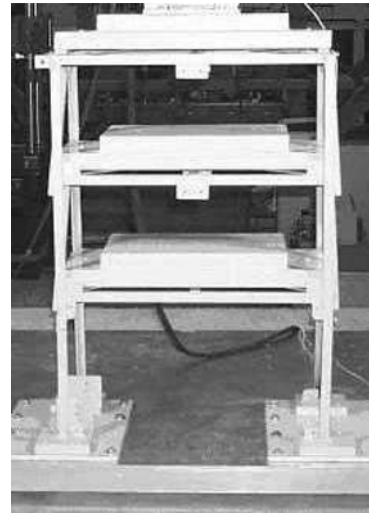

Fig. 2 Three story 1:10 scale building model

Table 1 Frequencies and damping ratios estimated using EMD/HT

Mode	Free vibration tests		White noise tests	
	Identified frequency (Hz)	Identified damping ratio (%)	Identified frequency (Hz)	Identified damping ratio (%)
1	5.5	1.9	5.5	1.5
2	18.7	1.0	18.7	1.0
3	34	1.1	33.7	1.0

the three modes as per the procedure described earlier in Section 3.2. The free vibration acceleration response of the third floor is shown in Fig. 4. The first three modes are not clearly evident in the time history as all three modes are present simultaneously and decay at different rates; hence, the need for time-frequency analysis exists to understand localization.

The EMD method is capable of extracting all the three vibration frequencies and damping ratios from a single measurement of the acceleration response time history based on the procedure outlined in Section 3.1. The third floor acceleration is decomposed into IMFs; the first three are shown in Fig. 5 and the rest are discarded as they are small and below the threshold. Based on the modal identification procedure presented in Section 3.1, modal frequencies and damping ratios are identified using linear least squares fit applied to the Hilbert Transform; log amplitude and phase (Eqs. 14, 43-47) of HT of IMF3 is shown in Fig. 6. The modal frequencies and damping ratios obtained are shown in Table 1.

IMFs of all three floor accelerations are obtained.

Magnitude/phase information of IMF3 of the three floor accelerations at a particular time, provides the first mode. Similarly second and third modes are obtained. The identified mode shapes (scaled to maximum of 1) are shown in Table 2. The analytical mode shapes are shown in Table 3. The EMD results are in agreement with the analytical results.

5.3 Validation of wavelet/HT technique using three story model free vibration test results

The three story scaled model is subjected to free vibration tests. The measured third floor free vibration displacement response signal is then analyzed using wavelets to extract instantaneous frequency and damping ratios of the three modes as per the procedure described in Section 4. The scalogram of the free vibration

Fig. 3   STFT of the measured third floor free vibration displacement response

Fig. 4   Measured third floor acceleration free vibration response
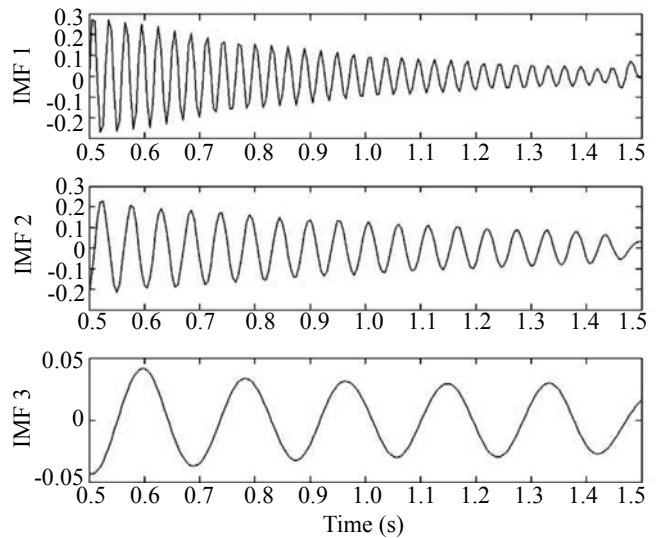
Fig. 5   IMF components of the third floor acceleration free vibration response
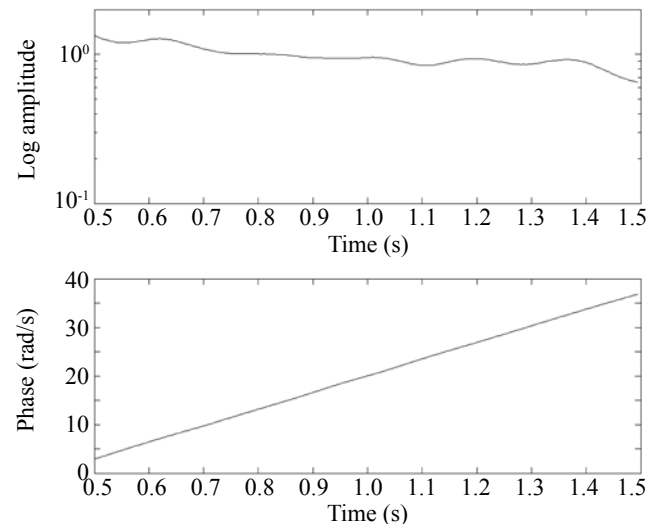
Fig. 6   HT of IMF3 of the third floor acceleration free vibration response

Table 2   Mode shapes estimated using EMD

	Mode-1	Mode-2	Mode-3
Storey-3	1.0000	-0.7025	-0.3787
Storey-2	0.6976	0.3265	1.0000
Storey-1	0.4696	1.0000	-0.6185

Table 3   Analytical mode shapes

	Mode-1	Mode-2	Mode-3
Storey-3	1.0000	-0.6416	-0.3946
Storey-2	0.6438	0.4299	1.0000
Storey-1	0.3648	1.0000	-0.6831

displacement response of the third floor is shown in Fig. 7 and relevant wavelet coefficients of the measured free vibration displacement response of all three floors and modes are shown in Fig. 8 (the wavelet coefficients have been normalized to have a peak value of 1 in mode 1). All three modes and their decrement as a function of time are clearly evident in Figs. 7 and 8. The modal frequencies and damping ratios are identified using

linear least squares fit applied to the Hilbert transform; log amplitude and phase (Eqs. (14), (43)–(47)) of HT of wavelet coefficient corresponding to mode 1 (Fig. 8 top) is shown in Fig. 9. The modal frequencies obtained are 5.5 Hz, 18.8 Hz, and 34 Hz, and the damping ratio of the first mode is estimated to be 1.9%; however, the damping in mode two and three are underestimated at 0.08%, as compared to the values shown in Table 1. Wavelet coefficients of all three floor displacements, shown in Fig. 8, are used to obtain the mode shapes. Magnitude/ phase information of wavelet coefficients of the three floor displacements at a particular time provides the first mode. The ratio of the wavelet coefficients shown in Fig. 8 remain nearly constant as a function of time. Similarly, the second and third modes are obtained.

The identified mode shapes (scaled to maximum of 1) are shown in Table 4. The analytical mode shapes are shown in Table 3. The wavelet results are in agreement with the analayatical results.

5.4 Validation of wavelet technique using numerical simulation of a 5DOF LTI system

A MDOF model is used to simulate the displacement
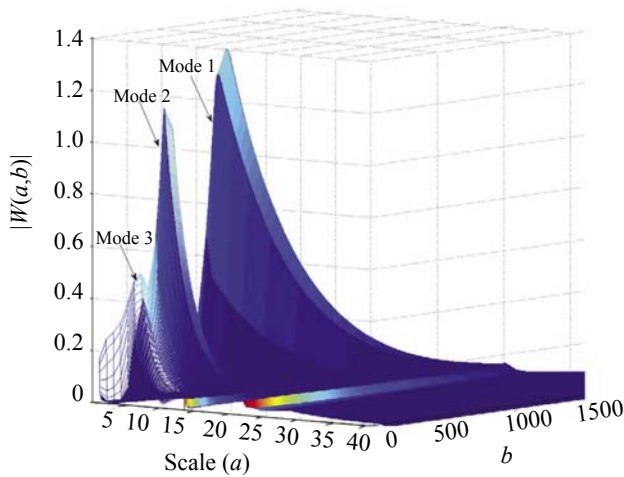
Fig. 7   Scalogram (view from below the x-y plane showing existence of three modes and free vibration decrement) of the measured third floor free vibration reponse
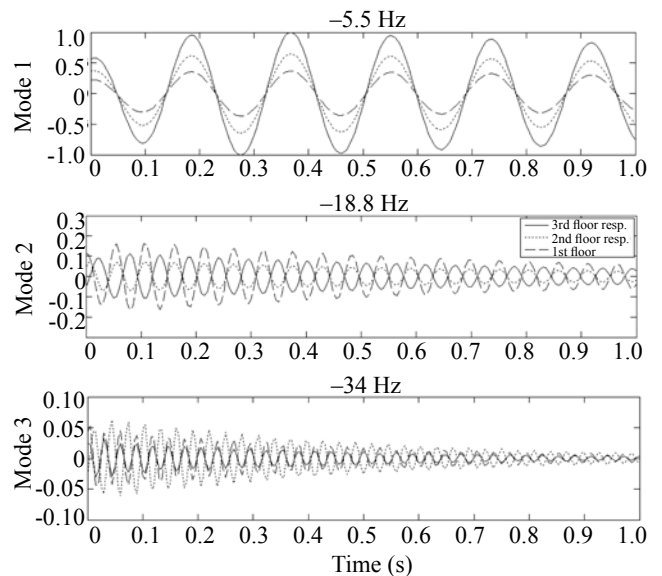

Fig. 8   Wavelet coefficients of the measured free vibration displacement response of all three floors

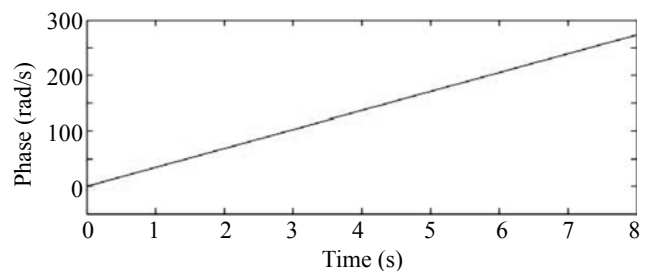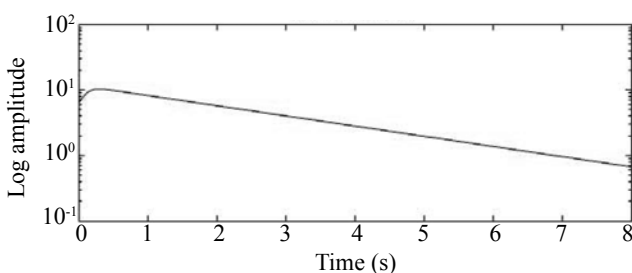**Fig. 9   First mode damping and frequency estimation using wavelet coefficient/Hilbert transform**

Table 4   Mode shapes estimated using wavelets

	Mode-1	Mode-2	Mode-3
Storey-3	1.0000	-0.6930	-0.3247
Storey-2	0.6437	0.4106	1.0000
Storey-1	0.3647	1.0000	-0.7475

response and to show the application of the proposed identification methodology. The MDOF system, as shown in Fig. 10, is considered. The displacement of the mass relative to the support is denoted $x_i(t)$. Simulation is carried out for a 5DOF system ($n = 5$). The masses are m_1= 300 kg, m_2= 200 kg, m_3= 200 kg, m_4= 250 kg and m_5= 350 kg; and the spring stiffnesses are k_1= 36 kN/m, k_2= 24 kN/m, k_3= 36 kN/m, k_4= 20 kN/mm and k_5= 15kN/mm respectively. The damping ratio is assumed to be 5% for all modes. The system is subjected to initial displacement of $x_i(0) = 1, i = 1, \cdots, 5$ for all the degrees of freedom. Using these, the ambient vibration response is simulated.

A modified L-P wavelet is used to decompose the signals into different frequency levels. Initially, the response energy is calculated for each degree of freedom in frequency bands with $\sigma = 2^{1/4}$ to broadly identify the bands that contain the natural frequencies. These bands are further divided into sub-bands using wavelet packets. Figures 8 and 10 represent the ratio of wavelet coefficients of displacements $x_i(t), i = 2, \cdots, 5$ with respect to the wavelet coefficients of displacement $x_1(t)$ over time for the five frequency sub-bands containing the five natural frequencies, respectively. Since the response for different degrees of freedom attain the same phase during modal vibration, these ratios are practically constant over time. The natural frequencies are estimated as the central frequency of the corresponding sub-bands and the corresponding mode shapes are obtained by averaging the ratios. The results for the first two modes are shown in Figs. 11 and 12 using sub-band coding as discussed in Section 4. The results are summarized in Table 5. Figures 13 and 14 show the mode shapes estimated using the proposed method and compared with the actual for the first three
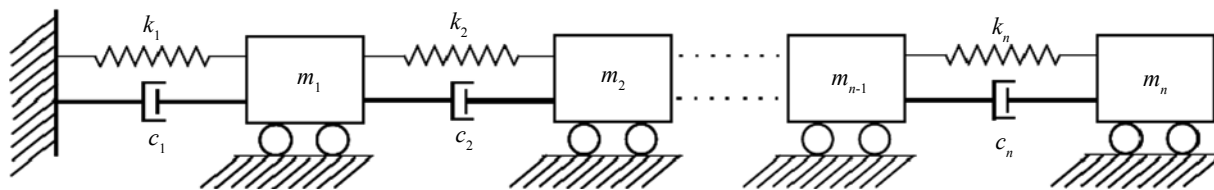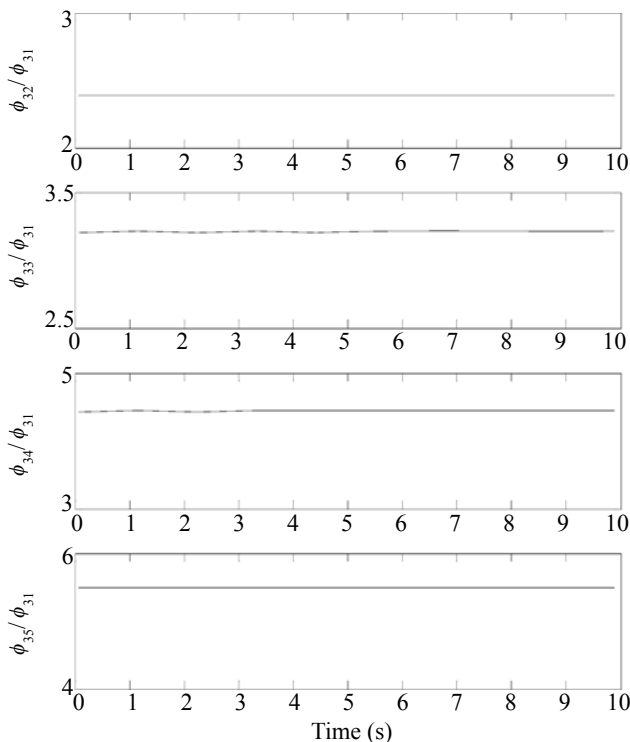

Fig. 10   MDOF system

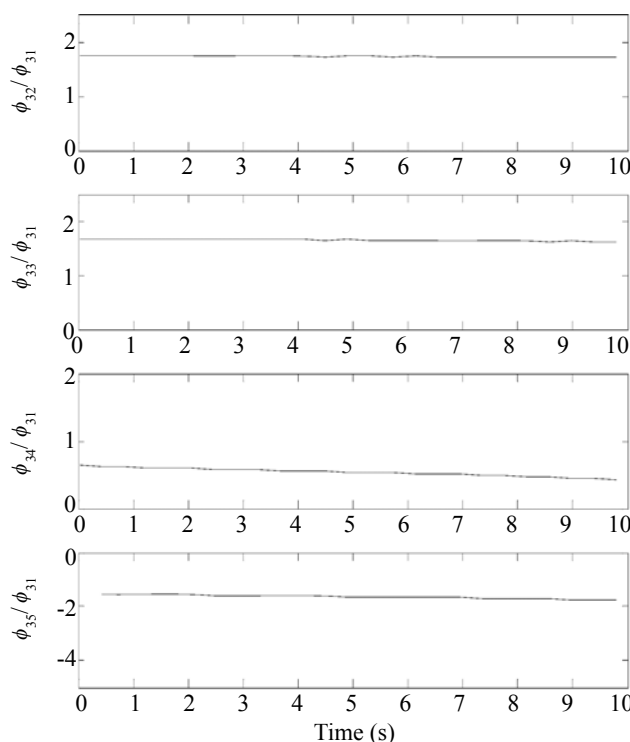**Fig. 11   Modal response at 1st natural frequency**

Fig. 12   Modal response at 2nd natural frequency

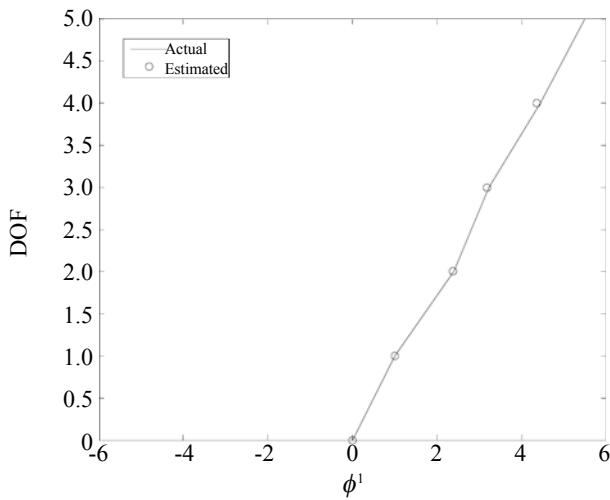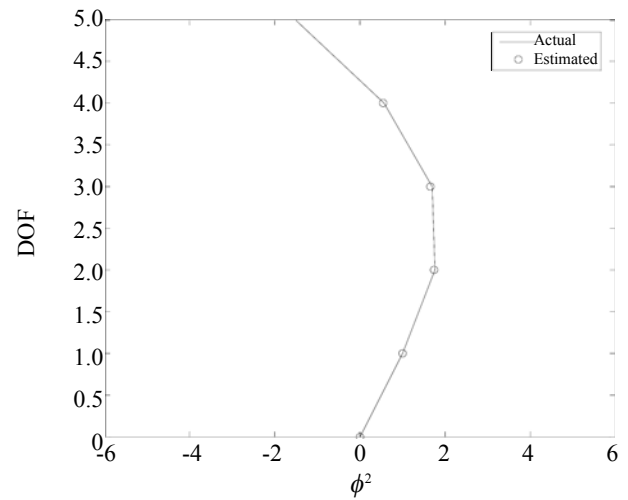**Fig. 13   First mode shape**

Fig. 14   Second mode shape

Table 5   Second mode shape estimated using wavelets

2*Mode	Natural frequency (rad/s)		Damping ratio (%)	
	Actual	Estimated	Actual	Estimated
1	2.84	2.88	0.05	0.04
2	7.69	7.69	0.05	0.03
3	12.35	12.59	0.05	0.02

Table 6   Third mode shape estimated using wavelets

3*Mode	Normalized mode shape								
	x_1	x_2	x_2	x_3	x_3	x_4	x_4	x_5	x_5
		Actual	Estimated	Actual	Estimated	Actual	Estimated	Actual	Estimated
1	1.00	2.40	2.37	3.22	3.18	4.45	4.39	5.48	5.39
2	1.00	1.76	1.73	1.69	1.66	0.56	0.69	-1.49	-1.58
3	1.00	0.59	0.89	-0.18	-0.59	-1.30	-1.02	0.51	0.63

modes, respectively. From Figs. 13 and 14 and Table 5, it can be noticed that the modal frequencies along with other modal parameters are estimated satisfactorily, which proves the effectiveness of the proposed method.

Although the ratios of wavelet coefficients for higher modes are constant over time, the accuracy in estimation reduces for the higher modes. This is due to the fact that the energy content in bands containing the higher modal frequencies reduces as the mode number increases.

For the 5DOF system, the estimation accuracies start deteriorating from the third mode onwards and are poorer for the last two modes. This indicates that more numbers of modes and the associated modal properties can be identified with greater accuracy, for systems with relatively greater number of degrees of freedom. Also, modal damping ratios can be estimated with reasonable accuracy, with the level of accuracy deteriorates with higher modes. The higher modal damping ratios tend to be underestimated.

5.5 Validation of wavelet technique using numerical simulation of a 2DOF LTV system

To demonstrate the application of the tracking methodology, an example of a 2DOF system has been considered. The system considered is a shear-building model. The masses at the first and second floors are m_1=10 unit and m_2=10 unit, respectively. The floor stiffness for the first and second floor are k_1=2500 unit and k_2=4500 unit, respectively. These parameters lead to the first and second natural frequencies, of ω_1=9.04 rad/s and ω_2=30.30 rad/s, respectively. The first and second mode shapes are $\{\Phi_{11},\Phi_{21}\}=\{1 \ 1.137\}$ and $\{\Phi_{12},\Phi_{22}\}=\{1 \ -0.048\}$, respectively. A band limited white noise excitation has been simulated. The range of frequencies is kept wide enough to cover the frequencies of the system to be identified. The excitation has been digitally simulated at a time step of $\Delta t = 0.0104$ s. The response of the system is simulated with 5% of

modal damping. For the frequency-tracking algorithm, a moving window of 400 time steps equal to 4.16 s has been chosen. For the identification of the 2DOF system, the parameters F_1 and σ are taken as 8.25rad/s and 1.2, respectively. To observe if the proposed method can track a sudden change in the stiffness of an MDOF system and follow the recovery to the original stiffness value(s), the stiffness k_1 and k_2 of the 2DOF are changed to 5000 unit and 5200 unit, respectively, at an instant of 5.72 s in time. Subsequently, the stiffnesses are restored to their original value at 12.48 s. During the changed phase, the natural frequencies and the mode shapes are changed to ω_1=11.57 rad/s; ω_2=35.11 rad/s; and $\{\Phi_{11},\Phi_{21}\}^t = \{1\ \ 1.157\}$; $\{\Phi_{12},\Phi_{22}\}^t = \{1\ \ -0.048\}$. Figures 15 and 16 show the tracked first natural frequency and the ratio of the first mode shape Φ_{21}/Φ_{11}. As expected, there is a time lag in tracking the frequency and mode shape. The change in the frequency is tracked in (three) steps corresponding to the bands of frequencies considered. To investigate if a relatively small change in stiffness can be tracked, a case where the natural frequency of a SDOF representing the first mode only changes from 9 rad/s to 9.5 rad/s is considered and the results for successful tracking are shown in Fig. 17 with a window width of 200 sampling points corresponding to a time delay of 2.08 s. For this, the parameters F1 and σ are taken as 8.9 rad/s and 1.02, respectively. This indicates that the minimum change in stiffness that can be tracked is related to the value of σ, and to identify a small change a relatively smaller value will be required.

5.6 Validation of wavelet & random decrement technique using three story model test results under white noise excitation: the case of structural damage detection

The three story scaled model was damaged intentionally to simulate structural deterioration (Nagarajaiah, 2009). The model was subjected to white noise tests before and after the structural damage. We choose 10 s of the measured acceleration record before damage and 10 s of the measured acceleration after damage. The measured third floor acceleration response signal is shown in Fig. 18, and the corresponding Fourier spectrum is shown in Fig. 19. From the Fourier spectrum, the first mode frequency evident is ~5.5 Hz, second mode frequency at ~18.8 Hz and third mode frequency at ~34 Hz. The lower first mode frequency after damage is evident. The scalogram of the acceleration response of the third floor is shown in Fig. 20 and relevant scaled wavelet coefficients of the measured third floor acceleration response are shown in Fig. 21. The first two wavelet coefficent time histories in Fig. 21 are the most interesting as they correspond to the first mode frequencies of 4.9 Hz (after damage) and 5.5 Hz (before damage). The first two wavelet coefficients in Fig. 21 detect the loss of stiffness at 10 s, as evident in the significant change at 10 s in both coefficients. The third and fourth time histories in Fig. 21 correspond to
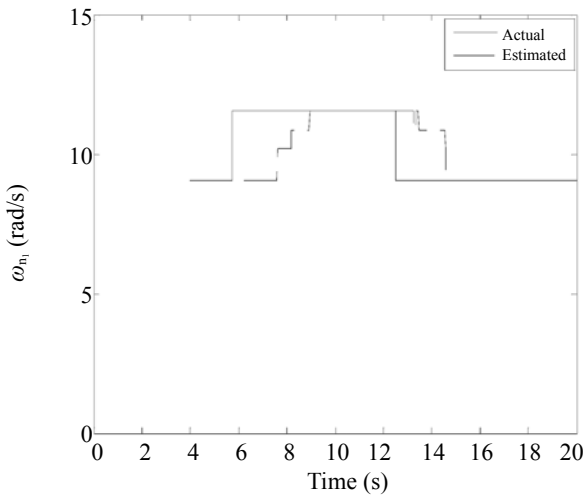

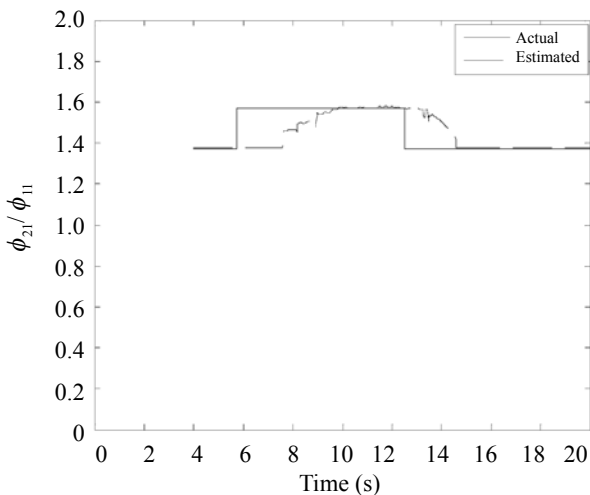**Fig. 15   Time varying first modal frequency**
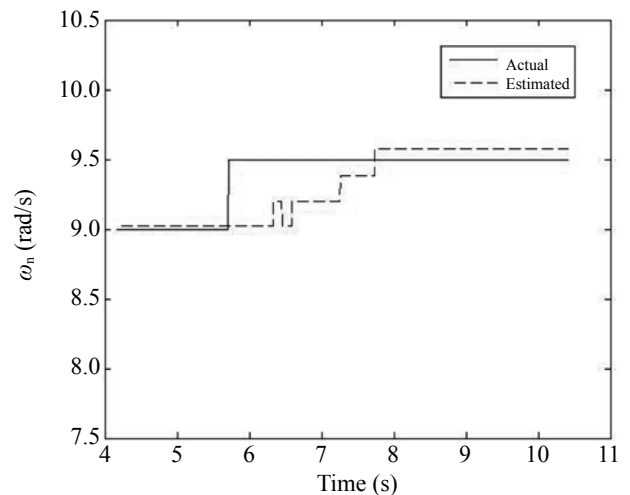

Fig. 16   Time varying first mode shape
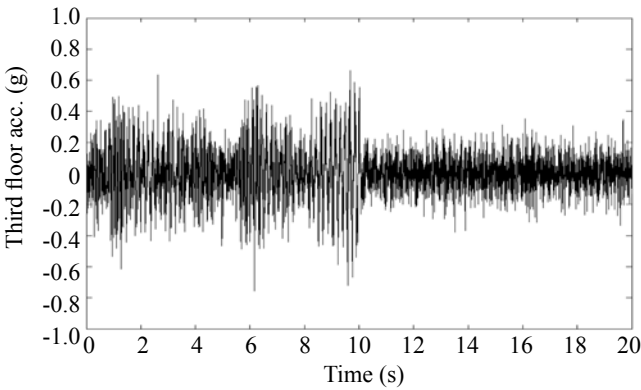

Fig. 17   Time varying frequency

Fig. 18　Measured third floor acceleration response to white noise excitation
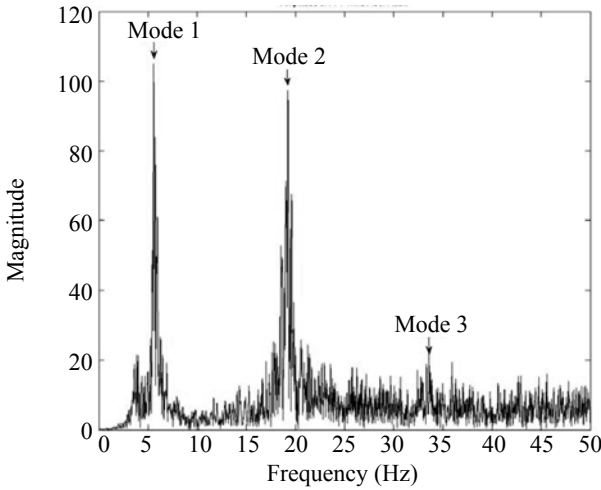

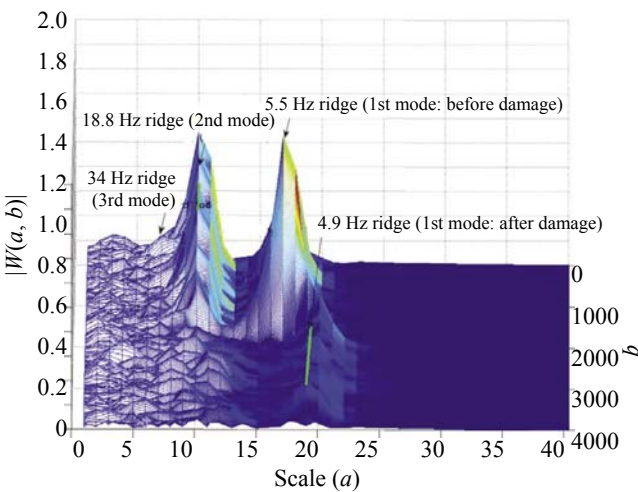**Fig. 19　Fourier spectrum of third floor acceleration**

Fig. 20　Scalogram of third floor acceleration response: note the shift in the first mode frequency (ridge) of 5.5 Hz to 4.9 Hz after 10 s due to damage
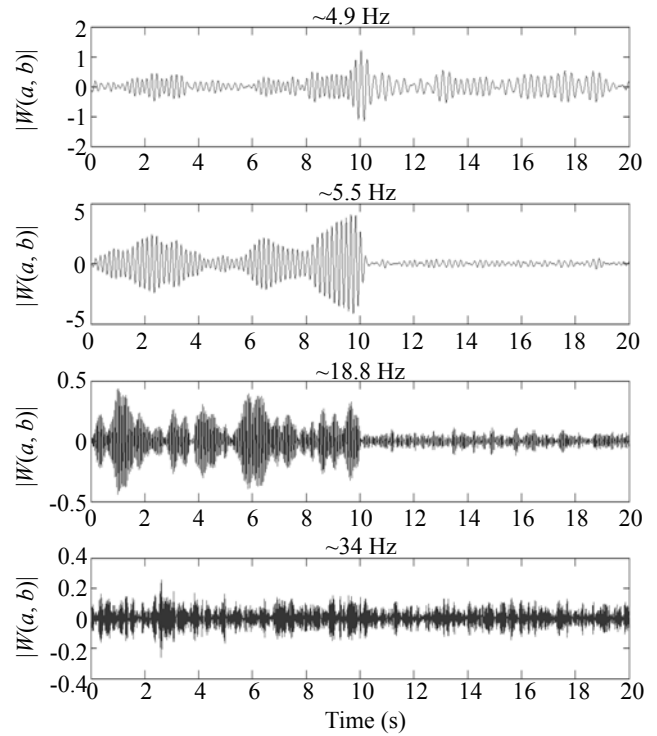

Fig. 21　Wavelet coefficients of the measured third floor acceleration response
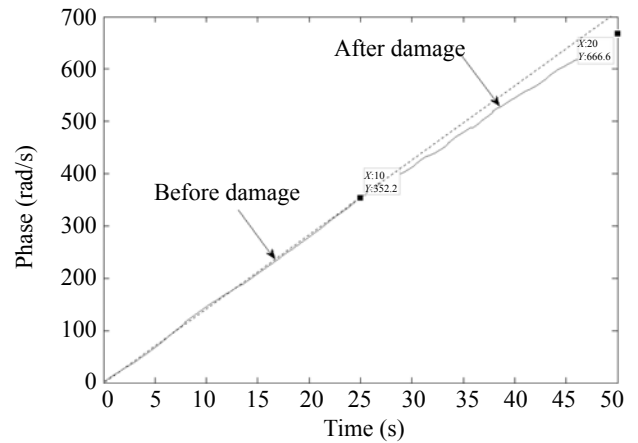

Fig. 22　First mode frequency estimation using wavelet coefficient/Hilbert transform (note the change in frequency before and after damage at 10 s)

third mode response does not indicate any change.

The modal frequency of the second wavelet coefficient in Fig. 21(b) is estimated using linear least squares fit applied to the Hilbert Transform; log amplitude and phase (Eqs. (14), (43)–(47)) of HT of the second wavelet coefficient corresponding to mode 1 before damage (Fig. 21(b)) is shown in Fig. 22. The change in frequency is clearly detected at 10 s; the frequency is ~5.5 Hz prior to damage and ~4.9 Hz after damage.

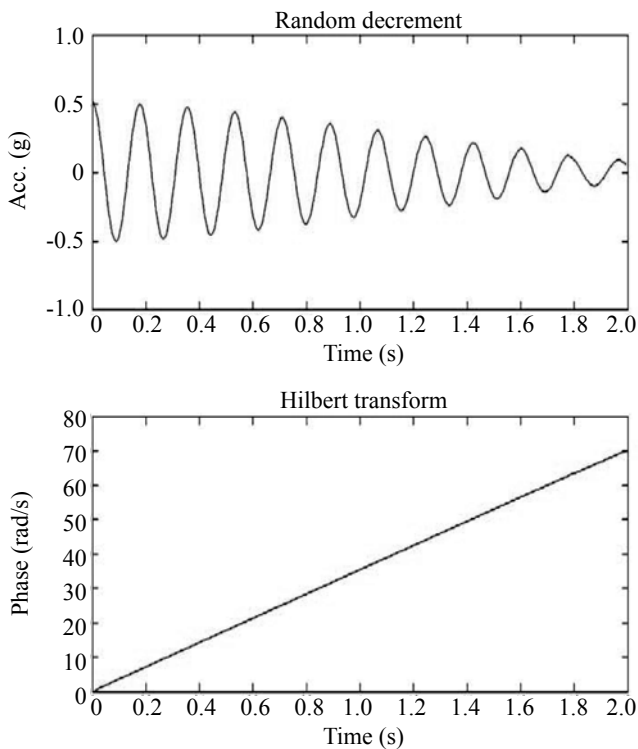The first two wavelet coefficient time histories in Fig. 21 are processed further to extract the free vibration

the second and third mode, respectively. Even the second mode response reduces at 10 s, although the frequency of the second mode does not change significantly. The

Fig. 23   First mode frequency estimation before damage using random decrement/HT
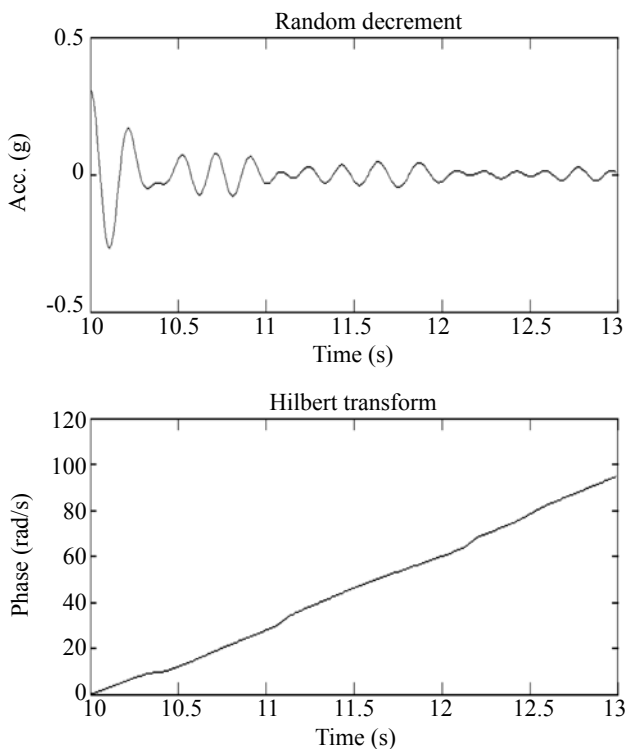

Fig. 24   First mode frequency estimation after damage using random decrement/HT

response using the random decrement technique. The third floor acceleration free vibration time history obtained from the random decrement technique before damage is shown in Fig. 23; also shown is the frequency estimation using HT—the estimated first mode frequency before damage is ~5.5 Hz. The third floor acceleration free vibration time history obtained from the random decrement technique after damage is shown in Fig. 24; also shown is the frequency estimation using HT—the estimated first mode frequency after damage is ~4.9 Hz. Damping ratios and mode shapes can be obtained as described in Section 4 (not shown due to space limitations).

5.7 Three story model test results under white noise excitation: STFT and EMD for structural damage detection

The third floor acceleration response was processed to white noise excitation using STFT and EMD. The spectrogram is shown in Fig. 25. The spectrogram detects the change in frequency from 5.5Hz to 4.9 Hz at 10 s. However, the fixed time-frequency resolution is a limitation that prevents robust detection when compared to the variable resolution of wavelets that enables more robust detection. In addition estimation of frequencies, damping ratios, and mode shapes would require further processing using band-pass filtering and Hilter transform apporach as described earlier in Section 3.

The third floor acceleration response was processed to white noise excitation using EMD. The IMFs are shown in Fig. 26. The IMFs do detect change at 10 s —particularly the IMF3 for the first mode before damage at 5.5 Hz; however, the detection is not as robust as in the case of the wavelet coefficients shown in Fig. 21.
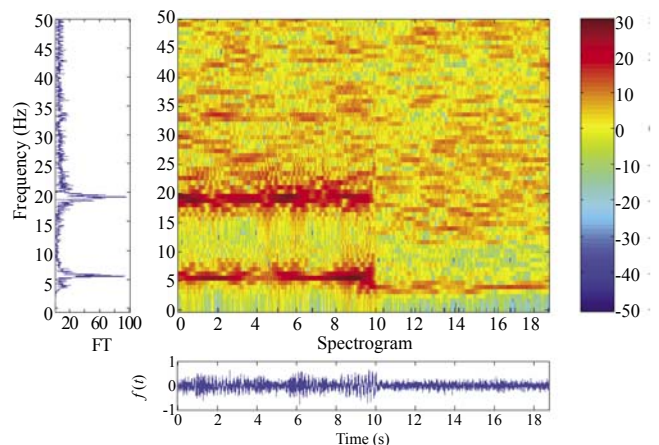

Fig. 25   Spectrogram of the third floor acceleration response to white noise excitation
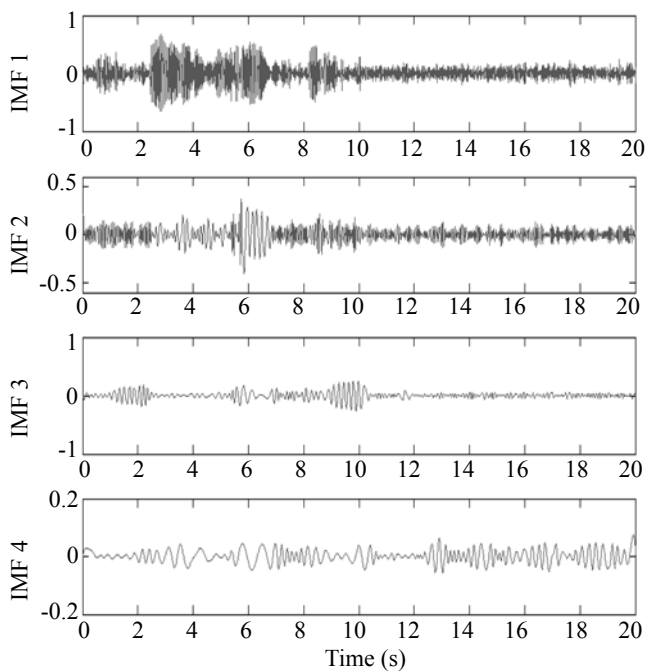
Fig. 26 IMFs of the third floor acceleration response to white noise excitation

6 Conclusions

The effectiveness of the developed time-frequency algorithms for output only modal identification of MDOF LTI and LTV systems has been demonstrated by simulated and experimental results. The algorithms presented demonstrate the powerful capabilities of time-frequency methods for output only modal identification and ease of implementation.

The STFT, EMD and wavelet, HT algorithms applied to MDOF LTI and LTV systems offer different advantages and limitations that can be summarized as follows.

(1) STFT based identification technique presented can detect the modal frequencies of LTI systems and their time localization very well; however, further processing using band-pass filtering is essential to obtain frequencies, damping ratios, and mode shapes. STFT can also detect changes in modal frequency of LTV systems due to structural damage. However, the fixed time-frequency resolution is a limitation that prevents robust detection when compared to the variable resolution of wavelets that enables more robust detection.

(2) The EMD based identification technique presented is capable of decomposing the free vibration or force vibration output signal into its individual modal components—represented by individual IMFs. Frequencies, damping ratios, and mode shapes of LTI systems can be obtained using the IMFs and the Hilbert transform approach. In case of ambient response, the random decrement technique can be used to obtain the free vibration response, followed by the application of EMD/HT for modal identification. The EMD technique

is capable of detecting changes in frequency of LTV systems due to structural damage; however, the detection may not be as robust as wavelets.

(3) The wavelet based identification technique presented is capable of extracting the modal components represented by wavelet coefficients obtained from the free vibration or forced vibration output response signals. Frequencies, damping ratios, and mode shapes of LTI and LTV systems can be obtained using wavelet coefficients and the Hilbert transform approach. In case of ambient response, the random decrement technique can be used to obtain the free vibration response, followed by the application of wavelet/HT for modal identification. The wavelet technique is very effective in detecting changes in frequency of LTV systems due to structural damage. The wavelet technique can also detect closely spaced modal frequencies and detect real time changes in frequencies and mode shapes of LTV systems.

7 Acknowledgement

References

Addison P, Watson JN and Feng T (2002), "Low-oscillation Complex Wavelets," *Journal of Sound and Vibration*, **254**(4): 733–762.

Agneni A and Balis-Cerma L (1989), "Damping Measurements from Truncated Signals via the Hilbert Transform," *Mechanical Systems and Signal Processing*, **3**(1): 1–3.

Al-Khalidy A, Noori M, Hou Z and Carmona R, "Yamamoto S, Masuda A and Sone A (1997), A Study of Health Monitoring Systems of Linear Structures Using Wavelet Analysis," *Approx Methods in the Design and Analysis of Pressure Vessels and Piping Components, ASME PVP*, **347**: 49–58.

Basu B (2005), "Identification of Stiffness Degradation in Structures Using Wavelet Analysis," *Construction and Building Materials*, **19**: 713–721.

Basu B (2007), "Assessment of Structural Integrity via Wavelet Based Time-frequency Analysis of Vibration Signals," *International Journal of Materials and Structural Integrity*, **1**: 238–258.

Basu B and Gupta VK (1997), "Non-stationary Seismic Response of MDOF Systems by Wavelet Modelling of

Non-stationary Processes," *Earthquake Engineering Structural Dynamics*, **26**: 1243–1258.

Basu B and Gupta VK (1998), "Seismic Response of SDOF Systems by Wavelet Modelling of Nonstationary Processes," *Journal of Engineering Mechaics*, ASCE, **124**(10): 1142–1150.

Basu B and Gupta VK (1999a), "On Equivalent Linearization Using Wavelet Transform," *Journal of Vibration and Acoustics*, ASME, **121**(4): 429–432.

Basu B and Gupta VK (1999b), "Wavelet Based Analysis of the Non-stationary Response of a Slipping Foundation," *Journal of Sound and Vibration*, **222**(4): 547–563.

Basu B and Nagarajaiah S (2008), "A Wavelet-based Time-varying Adaptive LQR Algorithm for Structural Control," *Engineering Structures*, Published on line March.

Basu B, Nagarajaiah S and Chakraborty A (2008), "Online Identification of Linear Time-varying Stiffness of Structural Systems by Wavelet Analysis," *International Journal of Structural Health Monitoring*, **7**(1): 21–36.

Chakraborty A, Basu B and Mitra M (2006), "Identification of Modal Parameters of a Mdof System by Modified L-P Wavelet Packets," *Journal of Sound and Vibration*, **295**(3–5): 827–837.

Chang CC and Chen LW (2003), "Vibration Damage Detection of a Timoshenko Beam by Spatial Wavelet Based Approach," *Applied Acoustics*, **64**: 1217–1240.

Chen B and Nagarajaiah S (2007), "Linear Matrix Inequality Based Robust Fault Detection and Isolation Using the Eigenstructure Assignment Method," *Journal of Guidance Control and Dynamics*, AIAA, **30**(6): 1831–1835.

Chen B and Nagarajaiah S (2008a), " $H\_/H_\infty$ Structural Damage Detection Filter Design Using Iterative LMI Approach," *Smart Materials and Structures*, **17**(3): Art. No. 035019.

Chen B and Nagarajaiah S (2008b), "Structural Damage Detection Using Decentralized Controller Design Method," *Smart Structures and Systems*, **4**(6): 779–794.

Cohen L (1995), *Time-frequency Analysis*, New Jersey: V Prentice –Hall.

Dharap P, Koh BH and Nagarajaiah S (2006), "Structural Health Monitoring Using ARMarkov Observers," *Journal of Intelligent Material Systems and Structures*, **17**(6): 469–481.

Feldman M (1994a), "Non-linear System Vibration Analysis Using Hilbert Transform — I. Free Vibration Analysis Method 'FREEVIB'," *Mechanical Systems and Signal Processing*, **8**(2): 119–127.

Feldman M (1994b), "Non-linear System Vibration Analysis Using Hilbert Transform-II. Forced Vibration Analysis Method 'ForceVib'," *Mechanical Systems and Signal Processing*, **8**(3): 309–318.

Gentile A and Messina A (2003), "On the Continuous Wavelet Transforms Applied to Discrete Vibrational Data for Detecting Open Cracks in Damaged Beams," *International Journal of Solids and Structures*, **40**: 295–315.

Ghanem R and Romeo F (2000), "A Wavelet Based Approach for the Identification of Linear Time-varying Dynamical Systems," *Journal of Sound and Vibration*, **4**: 555–576.

Ghanem R and Romeo F (2001), "A Wavelet Based Approach for Model and Parameter Identification of Nonlinear Systems," *International Journal of Nonlinear Mechanics*, **5**: 835–859.

Goggins J, Broderck BM, Basu B and Elghazouli AY (2006), "Investigation of Seismic Response of Braced Frames Using Wavelet Analysis," *Structural Control and Health Monitoring*, (in press, available online).

Gurley K and Kareem A (1999), "Applications of Wavelet Transforms in Earthquake, Wind and Ocean Engineering," *Engineering structures*, **21**(2): 149–167.

Hou Z, Nouri M and Amand R St (2000), "Wavelet Based Approach for Structural Damage Detection, *ASCE, Journal of Engineering Mechanics*, July 677–683.

Huang EN, Shen Z, Long RS, Wu CM, Shih HH, Zheng Q, Yen N, Tung CC and Liu HH (1998), "The Empirical Mode Decomposition and the Hilbert Spectrum for Nonlinear and Non-stationary Time Series Analysis," *Proc. Royal Soc. London*, **454**: 903–995.

Ibrahim SR (1977), "Random Decrement Technique for Modal Identification of Structures," *Journal of Spacecraft and Rockets*, **14**(11): 696-700.

Kijewski T and Kareem A (2003), "Wavelet Transforms for System Identification in Civil Engineering," *Computer-aided Civil and Infracstructure Engineering*, **18**(5): 339–355.

Kijewski-Correa T and Kareem A (2006), "Efficacy of Hilbert and Wavelet Transforms for Time-frequency Analysis," *Journal of engineering mechanics*, ASCE, **132**(10): 1037–1049.

Kijewski-Correa T and Kareem A (2007), "Performance of Wavelet Transform and Empirical Mode Decomposition in Extracting Signals Embedded in Noise," *Journal of engineering mechanics*, ASCE, **133**(7): 849–852.

Kitada Y (1998), "Identification of Nonlinear Structural Dynamic System Using Wavelet," *Journal of Engineering Mechanics*, ASCE, **124**(10): 1059–1066.

Koh BH, Dharap P and Nagarajaiah S (2005a), "Phan MQ. Real Time Structural Damage Monitoring by Input Error Function," *AIAA Journal*, **43**(8): 1808–1814.

Koh BH, Li Z, Dharap P, Nagarajaiah S and Phan MQ (2005b), "Actuator Failure Detection through Interaction Matrix Formulation," *Journal of Guidance Control and Dynamics*, AIAA, **28**(5): 895–901.

Koh BH, Nagarajaiah S and Phan MQ (2008), "Direct Identification of Structural Damage Through Kronecker Product Method," *Journal of Mechanical Science and Technology*, **22**(01): 103–112.

Kyprianou A and Staszewski WJ (1999), "On the Cross Wavelet Analysis of the Duffing Oscillator," *Journal of Sound and Vibration*, **228**(1): 119–210.

Lardies J and Gouttebroze S (2000), "Identification of Modal Parameters Using the Wavelet Transform," *International Journal of Mechanical Science*, **44**: 2263–2283.

Li Z, Koh BH and Nagarajaiah S (2007), "Detecting Sensor Failure via Decoupled Error Function and Inverse Input-output Model," *Journal of Engineering Mechanics*, ASCE, **133**(11): 1222–1228.

Liew KM and Wang Q (1998), "Application of Wavelet Theory for Crack Identification in Structures," *Amer. Soc. Civ. Eng, J. Eng. Mech.*, **124**(2): 152–157.

Loutridis S, Douka E and Trochidis A (2004), "Crack Identification in Double Cracked Beams Using Wavelet Analysis," *Journal of Sound and Vibration*, **277**: 1025–1039.

Melhem H and Kim H (2003), "Damage Detection in Concrete by Fourier and Wavelet Analysis," *Amer. Soc. Civ. Eng, J. Eng. Mech.*, **129**(5) 571–577.

Nagarajaiah S (2009), "Adaptive Passive, Semiactive, Smart Tuned Mass Dampers: Identification and Control Using Empirical Mode Decomposition, Hilbert Transform, and Short-term Fourier Transform," *Structural Control and Health Monitoring,* DOI: 10.1002 stc.349.

Nagarajaiah S and Dharap P (2003), "Reduced Order Observer Based Identification of Base Isolated Buildings," *Earthquake Engineering and Engineering Vibration*, **2**(2): 237–244.

Nagarajaiah S and Li Z (2004), "Time Segmented Least Squares Identification of Base Isolated Buildings," *Soil Dynamics and Earthquake Engineering Journal*, **24**, 577–586.

Nagarajaiah S and Sonmez E (2007), "Structures of Semiactive Variable Stiffness Multiple Tuned Mass Dampers Under Harmonic Forces," *Journal of Sructural Engineering*, ASCE, **133**(1): 67–77.

Nagarajaiah S and Varadarajan N (2001), "Semi-active Control of Smart Tuned Mass Damper Using Empirical Mode Decomposition and Hilbert Transform Algorithm," *Proc. ICOSSAR 2001, Newport Beach*, CA, June, CD ROM 2001.

Nagarajaiah S and Varadarajan N (2005), "Semi-active Control of Wind Excited Building with Variable Stiffness TMD Using Short Time Fourier Transform," *Engineering Structures*, **27**(3): 431–441.

Nagarajaiah S, Vardarajan N and Sahasrabudhe S (1999), "Variable Stiffness and Instantaneous Frequency," *Proc. Structures Congress*, ASCE, New Orleans, pp. 858–861.

Naldi G and Venini P (1997), "Wavelet Analysis of Structures: Statics, Dynamics and Damage Identification," *Meccanica*, **32**.

Narasimhan S and Nagarajaiah S (2005), "STFT Algorithm for Semiactive Control of Base Isolated Buildings with Variable Stiffness Isolation Systems Subjected to Near Fault Earthquakes," *Engineering structures*, **27**(4):514–523.

Newland DE (1993), *An Introduction to Random Vibrations, Spectral and Wavelet Analysis*, Longman, U.K.

Newland DE (1994a), "Wavelet Analysis of Vibration, Part1: Theory," *Trans. ASME Journal of Vibration and Acoustics*, **116**: 409–416.

Newland DE (1994b), "Wavelet Analysis of Vibration, Part2: Wavelet Maps," *Trans. ASME Journal of Vibration and Acoustics*, **116**: 417–425.

Okafor AC and Dutta A (2000), "Structural Damage Detection in Beams by Wavelet Transforms," *Smart Materials and Structures*, **9**: 906–917.

Pakrashi V, Basu B, and O'Connor A (2007), "Structural Damage Detection and Calibration Using Wavelet-Kurtosis Technique," *Engineering Structures*, (in press).

Patsias S and Staszewski WJ (2002), "Damage Detection Using Optical Measurements and Wavelets," *Structural Health Monitoring*, **1**(1): 5–22.

Patsias S, Staszewski WJ and Tomlinson GR (2002), "Image Sequences and Wavelets for Vibration Analysis. Part II – Extraction of Modal Damping and Modeshapes," *Proceedings of the Institution of Mechanical Engineers, Part C, Journal of Mechanical Engineering Science*, **216**(9): 901–912.

Piombo BAD and Fasana A, Marchesiello S and Ruzzene M (2000), "Modelling and Identification of the Dynamic Response of a Supported Bridge," *Mechanical Systems and Signal Processing*, **14**(1): 75–89.

Rilling G, Flandrin P and Goncalves P (2003), "On Empirical Mode Decomposition and Its Algorithms," *IEEE-EURASIP Workshop on Nonlinear Signal and Image Processing*, NSIP-03, Grado I.

Robertson A and Basu B (2008), "Wavelet Analysis," editors Boller C, Chang FK and Fujino Y, *Encyclopaedia on Structural Health Monitoring*, Wiley.

Robertson AN, Park KC and Alvin KF (1998), "Extraction of Impulse Response Data via Wavelet Transform for Structural System Identification," *J. Vib Acoustics*, ASME, **120**: 252–260.

Rucka M and Wilde K (2006), "Crack Identification Using Wavelets on Experimental Static Deflection Profiles," *Engineering Structures*, **28**: 279–288.

Ruzzene M, Fasana A, Garibaldi L and Piombo BAD (2000), "Natural Frequencies and Damping Identification Using Wavelet Transform: Application to Real Data," *Mechanical Systems and Signal Processing*,

11: 207–218.

Spanos PD, Failla G, Santini A and Pappatico M (2006), "Damage Detection in Euler-bernoulli Beam via Spatial Wavelet Analysis," *Structural Control and Health Monitoring*, **13**: 472–487.

Spencer B and Nagarajaiah S (2003), "State of the Art of Structural Control," *Journal of Structural Engineering,* ASCE, **129**(7): 845–856.

Staszewski WJ (1997), "Identification of Damping in MDOF Systems Using Time Scale Decomposition," *Journal of Sound and Vibration*, **203**: 283–305.

Staszewski WJ (1998a), "Identification of Non-linear Systems Using Multi-scale Ridges and Skeletons of the Wavelet Transform," *Journal of Sound and Vibration*, **214**(4): 639–658.

Staszewski WJ (1998b), "Structural and Mechanical Damage Detection Using Wavelets," *The Shock and Vibration Digest*, **30**(4): 457–472.

Staszewski WJ, Biemans C, Boller C and Tomlinson GR (1998), "Damage Detection Using Wavelet-based Statistical Analysis," *Proc of ISMA23*, **I**: 59–66.

Staszewski WJ and Robertson AN (2007), "Time-frequency and Time-scale Analysis for Structural Health Monitoring," *Philosophical Transactions of the Royal Society, Part A*, **365(1851)**: 449–477.

Staszewski WJ and Tomlinson GR (1994), "Application of the Wavelet Transform to Fault Detection in a Spur gear," *Mechanical Systems and Signal Processing*, **8:** 289–307.

Thrane N (1984), "The Hilbert transform," *Bruel & Kjaer Technical Review*, **3**.

Tomlinson GR (1987), "Developments in the Use of the Hilbert Transform for Detecting and Quantifying Non-Linearity Associated with Frequency Response Functions," *Mechanical Systems and Signal Processing*, **1**(2): 151–171.

Varadarajan N and Nagarajaiah S (2004), "Wind Response Control of Building with Variable Stiffness Tuned Mass Damper Using EMD/HT," *Journal of Engineering Mechanics*, ASCE, **130**(4): 451–458.

Wang Q and Deng X (1999), "Damage Detection with Spatial Wavelets," *International Journal of Solids and Structures*, **36**: 3443–3468.

Wang WJ and McFadden PD (1996), "Application of Wavelets to Gearbox Vibration Signals for Fault Detection," *Journal of Sound and Vibration*, **192**: 927–939.

Worden K and Tomlinson GR (2001), *Nonlinearity in Structural Dynamics*, Institute of Physics Publishing, Bristol and Philadelphia.

Yang JN, Lei Y, Lin S and Huang N (2004), Hilbert-haung Based Apporach for Structural Damage Detection," *Journal of Engineering Mechanics*, **130**(1): 85–95.

Yang JN, Lei Y, Pan S and Huang N (2003), System Identification of Linear Structures Based on Hilbert-Haung Spectral Analysis. Part I: Normal Modes," *Earthquake Engineering & Structural Dyanmics*, **32:** 1443–1467.

Zeldin BA and Spanos PD (1998), Spectral Identification of Nonlinear Structural Systems," *Journal of engineering mechanics*, ASCE, **124**(7): 728–733.